



**The Abdus Salam
International Centre for Theoretical Physics**



2132-13

Winter College on Optics and Energy

8 - 19 February 2010

**INTRODUCTION TO PHOTONIC CRYSTALS: NANOSTRUCTURED
MATERIALS
TO MANIPULATE LIGHT PROPAGATION & HARVESTING**

D. Comoretto
*Universita' di Genova
Italy*



INTRODUCTION TO PHOTONIC CRYSTALS: NANOSTRUCTURED MATERIALS TO MANIPULATE LIGHT PROPAGATION & HARVESTING

DAVIDE COMORETTO

*Dipartimento di Chimica e Chimica Industriale
Università di Genova*

comorett@chimica.unige.it



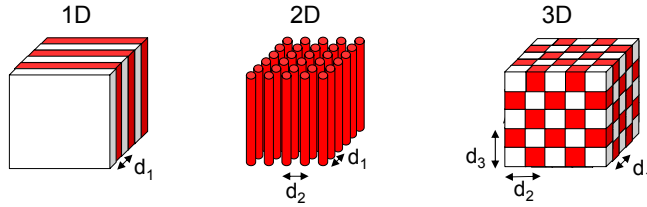
SUMMARY

INTRODUCTION TO PHOTONIC CRYSTALS: NANOSTRUCTURED MATERIALS TO MANIPULATE LIGHT PROPAGATION & HARVESTING

- **Photonic Crystals**
- Natural Photonic Crystals
- Growth & Preparation of Photonic Crystals
- Photonic Crystals Theory
- Photonic Crystals Applications
- Photonic Crystal in Photovoltaic Devices



PHOTONIC CRYSTALS



$d_j \gg a_0$ (Bohr's radius)
 $d_j \sim \lambda$ of visible light



The dielectric constant (ϵ) must be considered (dielectric lattice)

VOLUME 58, NUMBER 20

PHYSICAL REVIEW LETTERS

18 MAY 1987

Inhibited Spontaneous Emission in Solid-State Physics and Electronics

Eli Yablonovitch

Bell Communications Research, Navesink Research Center, Red Bank, New Jersey 07701

(Received 23 December 1986)

VOLUME 58, NUMBER 23

PHYSICAL REVIEW LETTERS

8 JUNE 1987

Strong Localization of Photons in Certain Disordered Dielectric Superlattices

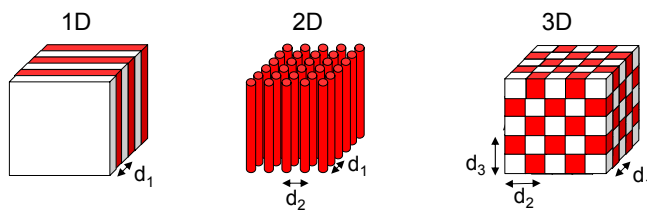
Sajeev John

Department of Physics, Princeton University, Princeton, New Jersey 08544

(Received 5 March 1987)



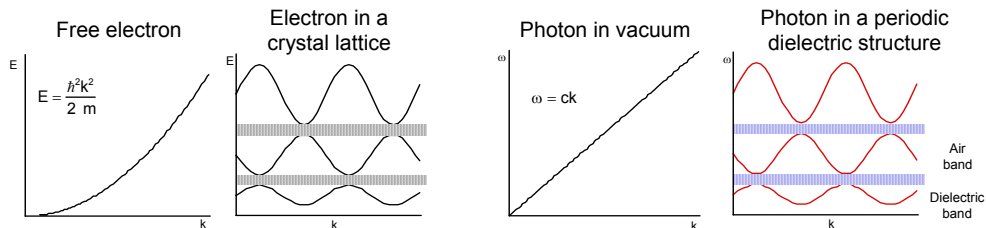
PHOTONIC CRYSTALS



$d_j \gg a_0$ (Bohr's radius)
 $d_j \sim \lambda$ of visible light

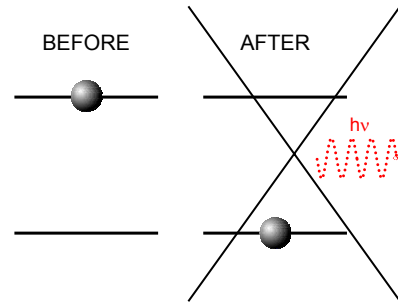
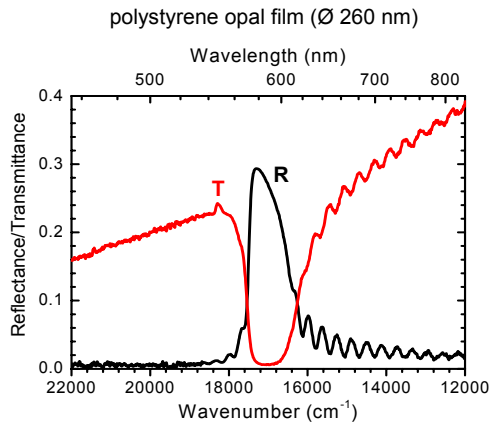


The dielectric constant (ϵ) must be considered (dielectric lattice)





OPTICAL EFFECTS OF PHOTONIC BAND GAP



Photons having energy within the band gap cannot propagate inside the photonic crystals thus being backward diffracted

Inhibition of spontaneous emission (Purcell's effect)



BAND GAP FORMATION

$$E = \frac{\hbar^2 K^2}{2m}$$

$$m\lambda = 2D \cos(\vartheta) = 2D \sqrt{1 - \sin^2(\vartheta)}$$

$$\psi_K = e^{iKx}$$

$$\omega = K \frac{c}{n}$$

$$m\lambda = 2D \sqrt{n_{\text{eff}}^2 - \sin^2(\vartheta)}$$

$$\psi_{\pm} = e^{iKx} \pm e^{-iKx}$$

The **electronic** band gap formation is due to the **electron waves** coherently scattered from **different potential regions**

The **photonic** band gap formation is due to the **electromagnetic fields** coherently scattered at the **interfaces between different dielectric regions**



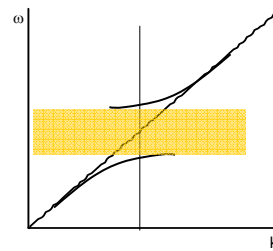
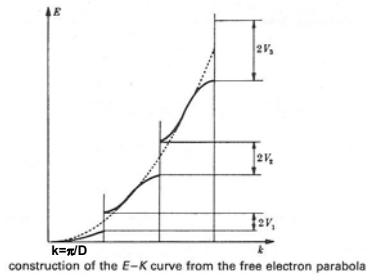
BAND GAP FORMATION

$$\psi_{\pm} = e^{ikx} \pm e^{-ikx}$$

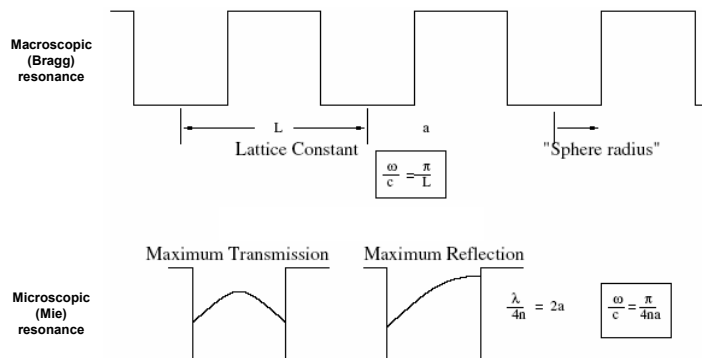
$$V_{\pm} = \frac{1}{L} \int |\psi_{\pm}|^2 V(x) dx = \pm V_n$$

Potential energy for the two waves is different ($V(x)$ Kronig-Penney potential), while kinetic one is unchanged

$$E_{\pm} = \frac{\hbar^2 K^2}{2m} \pm V_n$$



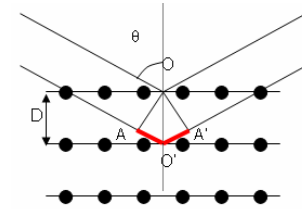
BAND GAP FORMATION



- A different way to explain the origin of the band gap concerns the role of Mie and Bragg scattering. The former is a microscopic process at the single repetition unit, while the latter involve the array.
- A photonic band gap appears when **the density of dielectric scatterers is such that the microscopic (Mie) scattering resonance of a single unit cell of the PC occurs at the same frequency as the macroscopic (Bragg) resonance of the periodic array.**
- The **Bragg** scattering condition is $\lambda = 2L$, where λ is the vacuum wavelength of light.
- **Mie** resonance in one dimension occurs when a quarter wavelength fits into a single well $\lambda/(4n) = 2a$.
- Combining these two conditions yields the optimal volume filling fraction $f \equiv 2a/L = 1/(2n)$.

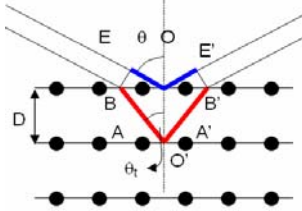


BAND GAP: BRAGG-SNELL LAW



$$m\lambda = 2D\cos\theta = 2D\sqrt{1-\sin^2\theta} \quad \text{Bragg's law}$$

$$n_i \sin\theta_i = n_t \sin\theta_t \quad \text{Snell's law}$$



$$m\lambda = 2D\sqrt{n_{\text{eff}}^2 - \sin^2\theta} \quad \text{Bragg-Snell law}$$



SUMMARY

INTRODUCTION TO PHOTONIC CRYSTALS: NANOSTRUCTURED MATERIALS TO MANIPULATE LIGHT PROPAGATION & HARVESTING

- Photonic Crystals
- **Natural Photonic Crystals**
- Growth & Preparation of Photonic Crystals
- Photonic Crystals Theory
- Photonic Crystals Applications
- Photonic Crystal in Photovoltaic Devices



NATURAL PHOTONIC CRYSTALS



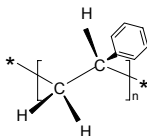
- Natural photonic crystals are mainly due to self-organization: suitable building blocks self-assemble in mesomorphic structures.
- Such structures might have different degree of order and this affects both the optical response of the system as well as the associated biological function.



EFFECT OF NANOSTRUCTURE ON THE TRANSPARENCY OF POLYSTYRENE

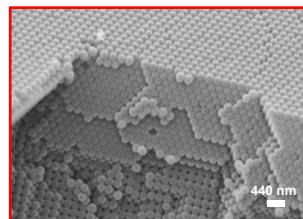
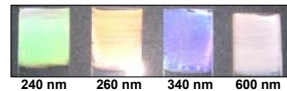
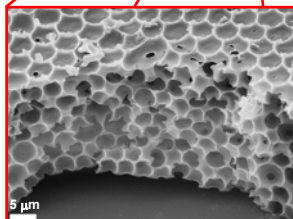


Transparent amorphous polystyrene



Highly diffusing (white) microstructured polystyrene film cast from CS₂ solutions in a wet environment

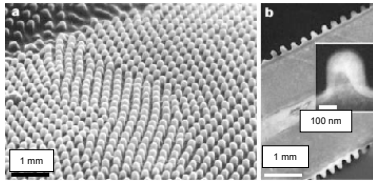
M. Civardi et al., Langmuir 21, 3480 (05)



Colloidal opal photonic crystal (iridescent) grown by vertical deposition of monodisperse polystyrene microspheres



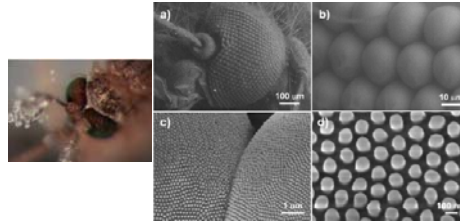
NANOSTRUCTURED MEDIA IN NATURE



Anti-reflecting ripple arrays on (a) arthropod ommatidia and (b) transparent wings of a diurnal moth.

Nanostructures allow to tune the refractive index from bulk to air in a continuous way thus reducing dielectric contrast and then reflection

P. Vukusic and J.R. Sambles, Nature 424, 852 (2003)



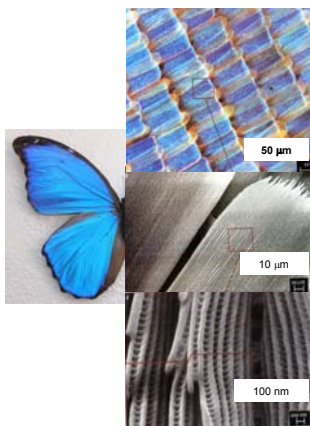
Compound eyes of the mosquito *C. pipiens* possess ideal superhydrophobic properties that provide an effective protective mechanism for maintaining clear vision in a humid habitat. This unique property is attributed to elaborate micro- and nano-structures:

- hexagonally close-packed (hcp) ommatidia at the **microscale** efficiently **prevent fog droplets trapping** in the voids between the ommatidia.
- hexagonally non-close-packed (ncp) nipples at the **nanoscale** **prevent microscale fog droplets condensation** on the ommatidia surface

X. Gao et al. Adv. Mater. 19, 2213 (2007)



NATURAL PHOTONIC CRYSTALS



Butterfly wings
“Morpho”

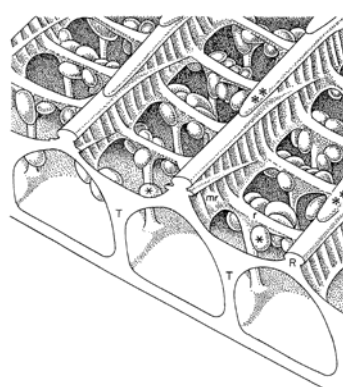
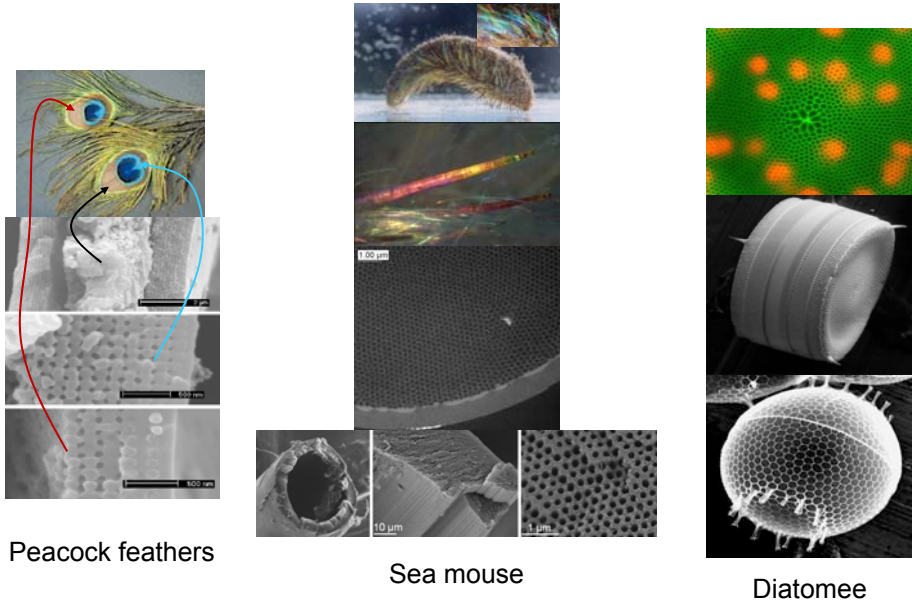


Fig. 3. Diagrammatic representation of part of a fractured scale showing the relationship between the lower lamina, trabeculae (T), ridges (R), lamellae (**), ribs (r), and microtubules (m). This view also shows pigment granules (*), not present in all scales.



NATURAL PHOTONIC CRYSTALS



Peacock feathers

Sea mouse

Diatomee



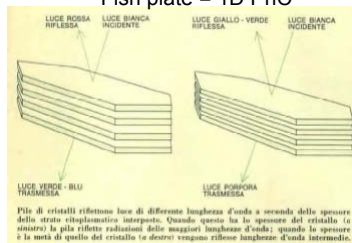
A PHOTONIC CRYSTAL FISH

I riflettori dei pesci

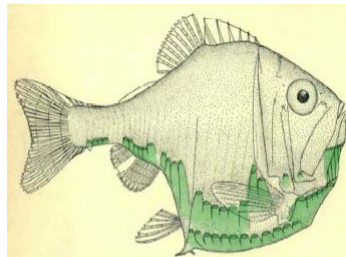
Molti pesci producono sostanze azotate che cristallizzano in strati riflettenti speculari. Nelle squame e sulla pelle questi strati hanno funzione ornamentale e mimetica; in altri casi migliorano la visione

Le Scienze 32, 92 (1971)
di Eric Denton

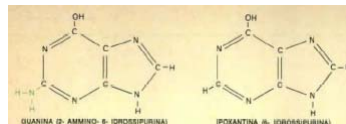
Fish plate = 1D PhC



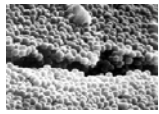
Pila di cristalli riflette luce di differente lunghezza d'onda a seconda delle spessore dello strato cristallino interposto. Quando spesse ha lo spessore del cristallo (a sinistra) la pila riflette radiazioni delle maggiori lunghezze d'onda; quando la spessore è la metà di quello del cristallo (a destra) vengono riflesse lunghezze d'onda intermedie.



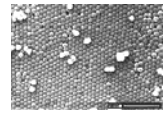
Pesce pescato dalla specie *Argopecten vulcanus* studiato dall'autore a bordo della nave oceanografica *Discovery*. Il pesce misura circa 7 cm; una serie di listelli diretti verso il basso corre dal capo alla coda, prevalentemente nella regione ventrale.



- 1D PhC: multilayer composed of molecular crystals layers ($n_1=1.8$) alternate to cytoplasm ($n_2=1.33$).
- High reflectance is observed since $\lambda/4$ condition is achieved ($\lambda/4=n_1d_1=n_2d_2$).



OPAL STRUCTURE AND PHOTONIC CRYSTALS



December 19, 1964 NATURE 1151

COLOUR OF PRECIOUS OPAL

By Dr. L. V. SANDERS

Communications University and Industrial Research Organization, Division of Technology, University of Melbourne

SOURCE: Australian opals are considered for the purposes of this paper to be spheres of silica which they contain. They are distinguished from other precious opals, and are related to other opals.

It is known that the colour from precious opals are caused by diffraction, and it is commonly assumed that they are caused by "diffraction rather than interference". The 1922 Bragg's model was an extensive optical investigation of these opals, and concluded that they were produced by a regular structure. Later, it was recognized that such diffraction opals were made up of regularly spaced layers of one type of silica with different refractive indices. However, the work outlined here using electron microscopy has shown that, in fact, the colour are caused by diffraction from a regular three-dimensional structure arising from the regular packing of spherical particles of silica, from opals & transparent opals.

These opals are better and more regular in structure than those of a regular three-dimensional lattice of spheres. The spheres are of a regular size of approximately 200 nm in diameter, and are arranged in a regular lattice. The spheres are arranged in a regular lattice, and are arranged in a regular lattice. The spheres are arranged in a regular lattice, and are arranged in a regular lattice.

Fig. 1. Section of an opal showing the lattice of silica spheres.

Fig. 2. Section of an opal showing the lattice of silica spheres.

Fig. 3. Section of an opal showing the lattice of silica spheres.

Fig. 4. Section of an opal showing the lattice of silica spheres.

Fig. 5. Section of an opal showing the lattice of silica spheres.

Fig. 6. Section of an opal showing the lattice of silica spheres.

Fig. 7. Section of an opal showing the lattice of silica spheres.

Fig. 8. Section of an opal showing the lattice of silica spheres.

Fig. 9. Section of an opal showing the lattice of silica spheres.

Fig. 10. Section of an opal showing the lattice of silica spheres.

Fig. 11. Section of an opal showing the lattice of silica spheres.

Fig. 12. Section of an opal showing the lattice of silica spheres.

Fig. 13. Section of an opal showing the lattice of silica spheres.

Fig. 14. Section of an opal showing the lattice of silica spheres.

Fig. 15. Section of an opal showing the lattice of silica spheres.

Fig. 16. Section of an opal showing the lattice of silica spheres.

Fig. 17. Section of an opal showing the lattice of silica spheres.

Fig. 18. Section of an opal showing the lattice of silica spheres.

Fig. 19. Section of an opal showing the lattice of silica spheres.

Fig. 20. Section of an opal showing the lattice of silica spheres.

Fig. 21. Section of an opal showing the lattice of silica spheres.

Fig. 22. Section of an opal showing the lattice of silica spheres.

Fig. 23. Section of an opal showing the lattice of silica spheres.

Fig. 24. Section of an opal showing the lattice of silica spheres.

Fig. 25. Section of an opal showing the lattice of silica spheres.

Fig. 26. Section of an opal showing the lattice of silica spheres.

Fig. 27. Section of an opal showing the lattice of silica spheres.

Fig. 28. Section of an opal showing the lattice of silica spheres.

Fig. 29. Section of an opal showing the lattice of silica spheres.

Fig. 30. Section of an opal showing the lattice of silica spheres.

Fig. 31. Section of an opal showing the lattice of silica spheres.

Fig. 32. Section of an opal showing the lattice of silica spheres.

Fig. 33. Section of an opal showing the lattice of silica spheres.

Fig. 34. Section of an opal showing the lattice of silica spheres.

Fig. 35. Section of an opal showing the lattice of silica spheres.

Fig. 36. Section of an opal showing the lattice of silica spheres.

Fig. 37. Section of an opal showing the lattice of silica spheres.

Fig. 38. Section of an opal showing the lattice of silica spheres.

Fig. 39. Section of an opal showing the lattice of silica spheres.

Fig. 40. Section of an opal showing the lattice of silica spheres.

Fig. 41. Section of an opal showing the lattice of silica spheres.

Fig. 42. Section of an opal showing the lattice of silica spheres.

Fig. 43. Section of an opal showing the lattice of silica spheres.

Fig. 44. Section of an opal showing the lattice of silica spheres.

Fig. 45. Section of an opal showing the lattice of silica spheres.

Fig. 46. Section of an opal showing the lattice of silica spheres.

Fig. 47. Section of an opal showing the lattice of silica spheres.

Fig. 48. Section of an opal showing the lattice of silica spheres.

Fig. 49. Section of an opal showing the lattice of silica spheres.

Fig. 50. Section of an opal showing the lattice of silica spheres.

Fig. 51. Section of an opal showing the lattice of silica spheres.

Fig. 52. Section of an opal showing the lattice of silica spheres.

Fig. 53. Section of an opal showing the lattice of silica spheres.

Fig. 54. Section of an opal showing the lattice of silica spheres.

Fig. 55. Section of an opal showing the lattice of silica spheres.

Fig. 56. Section of an opal showing the lattice of silica spheres.

Fig. 57. Section of an opal showing the lattice of silica spheres.

Fig. 58. Section of an opal showing the lattice of silica spheres.

Fig. 59. Section of an opal showing the lattice of silica spheres.

Fig. 60. Section of an opal showing the lattice of silica spheres.

Fig. 61. Section of an opal showing the lattice of silica spheres.

Fig. 62. Section of an opal showing the lattice of silica spheres.

Fig. 63. Section of an opal showing the lattice of silica spheres.

Fig. 64. Section of an opal showing the lattice of silica spheres.

Fig. 65. Section of an opal showing the lattice of silica spheres.

Fig. 66. Section of an opal showing the lattice of silica spheres.

Fig. 67. Section of an opal showing the lattice of silica spheres.

Fig. 68. Section of an opal showing the lattice of silica spheres.

Fig. 69. Section of an opal showing the lattice of silica spheres.

Fig. 70. Section of an opal showing the lattice of silica spheres.

Fig. 71. Section of an opal showing the lattice of silica spheres.

Fig. 72. Section of an opal showing the lattice of silica spheres.

Fig. 73. Section of an opal showing the lattice of silica spheres.

Fig. 74. Section of an opal showing the lattice of silica spheres.

Fig. 75. Section of an opal showing the lattice of silica spheres.

Fig. 76. Section of an opal showing the lattice of silica spheres.

Fig. 77. Section of an opal showing the lattice of silica spheres.

Fig. 78. Section of an opal showing the lattice of silica spheres.

Fig. 79. Section of an opal showing the lattice of silica spheres.

Fig. 80. Section of an opal showing the lattice of silica spheres.

Fig. 81. Section of an opal showing the lattice of silica spheres.

Fig. 82. Section of an opal showing the lattice of silica spheres.

Fig. 83. Section of an opal showing the lattice of silica spheres.

Fig. 84. Section of an opal showing the lattice of silica spheres.

Fig. 85. Section of an opal showing the lattice of silica spheres.

Fig. 86. Section of an opal showing the lattice of silica spheres.

Fig. 87. Section of an opal showing the lattice of silica spheres.

Fig. 88. Section of an opal showing the lattice of silica spheres.

Fig. 89. Section of an opal showing the lattice of silica spheres.

Fig. 90. Section of an opal showing the lattice of silica spheres.

Fig. 91. Section of an opal showing the lattice of silica spheres.

Fig. 92. Section of an opal showing the lattice of silica spheres.

Fig. 93. Section of an opal showing the lattice of silica spheres.

Fig. 94. Section of an opal showing the lattice of silica spheres.

Fig. 95. Section of an opal showing the lattice of silica spheres.

Fig. 96. Section of an opal showing the lattice of silica spheres.

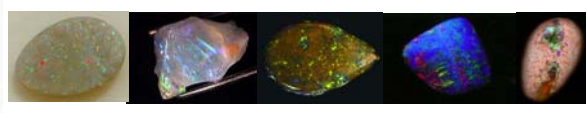
Fig. 97. Section of an opal showing the lattice of silica spheres.

Fig. 98. Section of an opal showing the lattice of silica spheres.

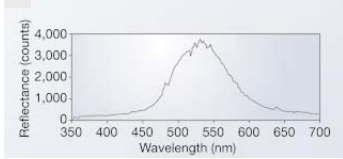
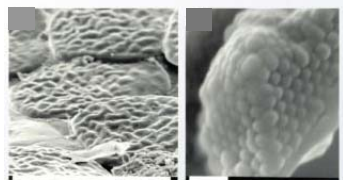
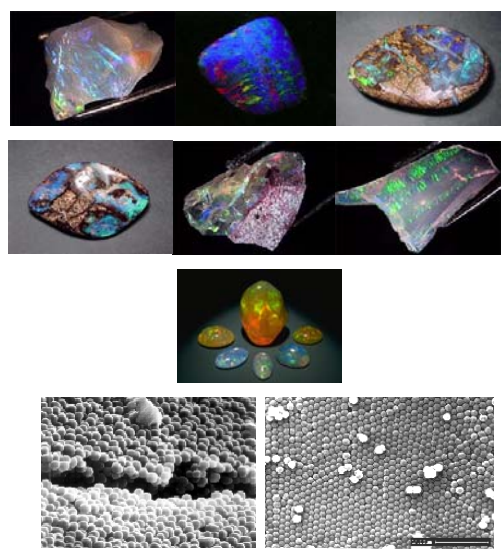
Fig. 99. Section of an opal showing the lattice of silica spheres.

Fig. 100. Section of an opal showing the lattice of silica spheres.

- Name of the products derived from natural ageing of silica hydrogels under high pressure and temperature.
- Sanders, showed the structure of opals and provided a rough explanation for their colors.
- From the Old Greek **οπαλλος** "To see the changing of the color".
- From the Latin **OPALLUS**, derived from the Sanskrit "Gem stone".



NATURAL AND ARTIFICIAL OPALS





SUMMARY

INTRODUCTION TO PHOTONIC CRYSTALS: NANOSTRUCTURED MATERIALS TO MANIPULATE LIGHT PROPAGATION & HARVESTING



- Photonic Crystals
- Natural Photonic Crystals
- Growth & Preparation of Photonic Crystals
- Photonic Crystals Theory
- Photonic Crystals Applications
- Photonic Crystal in Photovoltaic Devices



PHOTONIC CRYSTALS GROWTH

TOP-DOWN

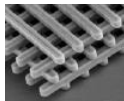
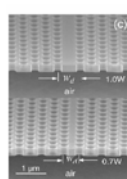
Bulk materials are carved to obtain the periodic dielectric constant nano-structure.

- Selective etching of the substrate below a mask.  **2D**
- Electron beam or X-ray lithographic techniques.  **3D**
- Two-photon polymerization

1D

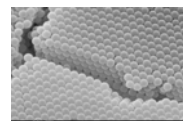
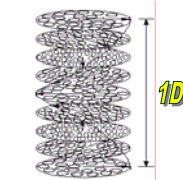
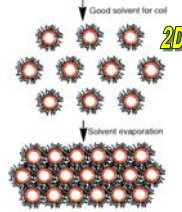
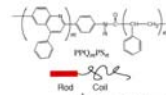
2D

3D



BOTTOM-UP

The photonic crystal is grown by self-assembly of both nano-units (e.g. spheres) or supramolecular aggregates (cholesteric liquid crystals, multi-block copolymers).



Science 283, 372 (99)



TWO-PHOTON POLYMERIZATION FOR 3D-MICROFABRICATION AND DEFECT-WRITING

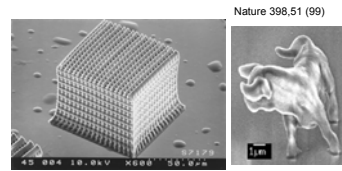
Two-photon excitation provides a means of activating chemical or physical processes with high spatial resolution in 3D and has made possible the development of

- 3D Fluorescence imaging
- Optical data storage
- Lithographic microfabrication.

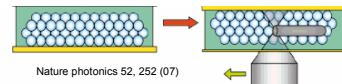
$$\text{TPA} \div I_{\text{laser}}^2$$

$$\text{TPA}_{\text{volume}} \div \lambda_{\text{laser}}^3$$

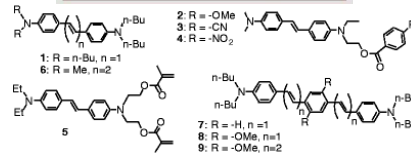
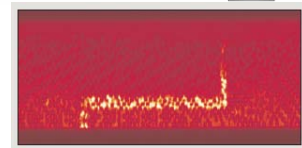
Photo-chemical reaction are confined to $\text{TPA}_{\text{volume}}$ small volumes



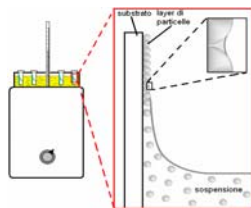
Nature 398,51 (99)



Nature photonics 52, 252 (07)



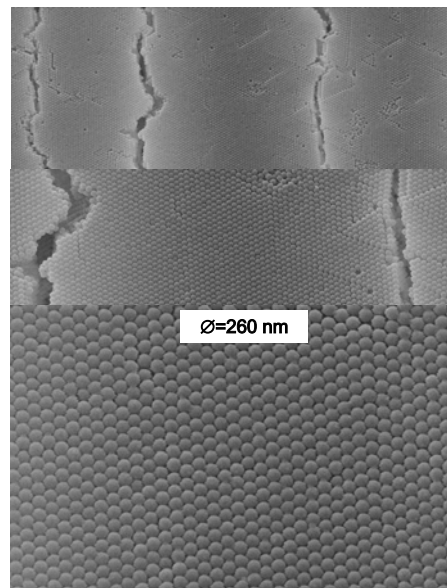
ARTIFICIAL OPALS



- T=55°C
- μ -sphere concentration 0,05%



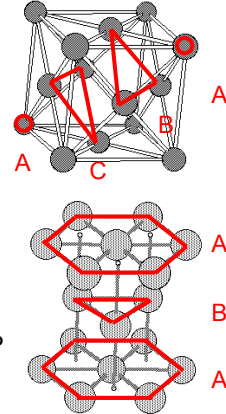
- T=45°C
- μ -sphere concentration 0,025%





HARD SPHERES PACKING

- Freezing of hard spheres is one of the most dramatic illustrations that crystalline order can be entropy driven.
- the FCC (ABCABC...) phase is more stable than HCP (ABABAB...) one by $9 \pm 2 \cdot 10^{-4} K_B T$ per particle.
- As the free-energy difference between the two phases is very small, the spontaneous generation of stacking faults is quite common (randomly stacked hexagonal close-packed, RHCP, crystallites).



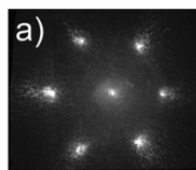
To estimate the rate at which the FCC phase grows from the RHCP phase, we need to estimate the relative free energy:

- The difference in bulk free energies per particle of the pure FCC and HCP phases, $\Delta f = f_{\text{HCP}} - f_{\text{FCC}}$.
- The interfacial free energy $\gamma_{\text{HCP-FCC}}$, which is the measure of the additional free-energy cost to create an FCC-HCP interface.
- The stacking entropy of the RHCP phase ($K_B \ln 2$ per plane).

Phys. Rev. Lett. 63, 2753 (89)
Phys. Rev. Lett. 79, 3002 (97)

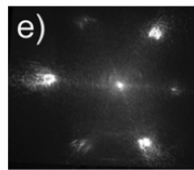


LIGHT DIFFRACTION TO PROBE ORDER



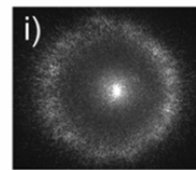
1 layers

All spots have same intensity (H)



6 layers

2 different set of spot intensity (FCC)

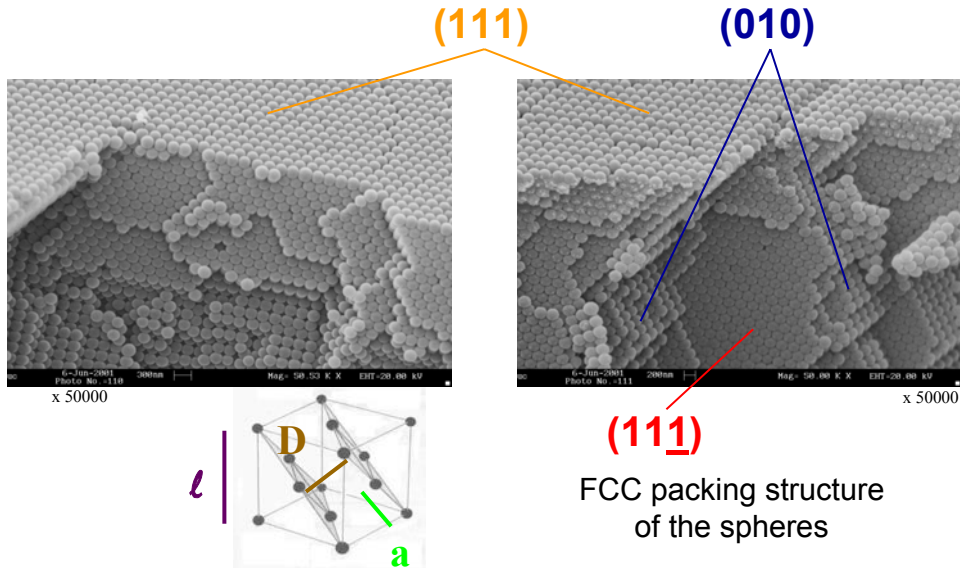


Disordered

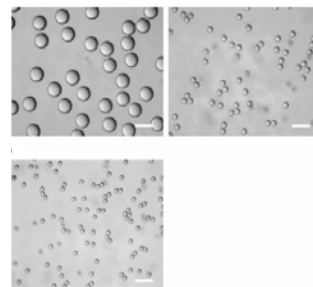
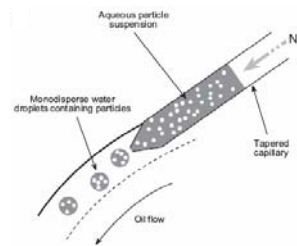
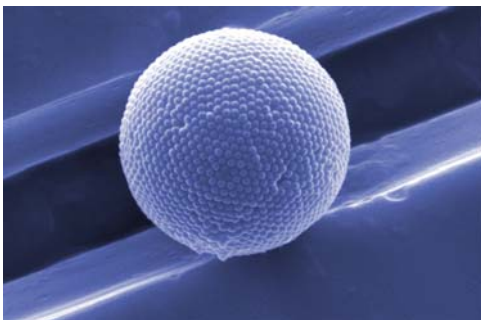
Powder-like diffraction



SEM OF POLYSTYRENE BULK OPALS



SPHERICAL OPALS: PHOTONIC BALLS





POLYMER MULTILAYERS

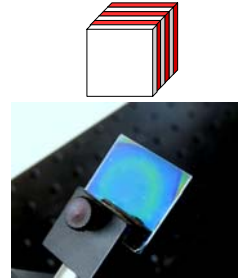
Polymeric multilayer films have been manufactured via three main methods:

co-extrusion, spin coating, and self-assembly.

Co-extruded films containing large numbers of alternating layers of different refractive indices were produced over 30 years ago at Dow, with first order reflectivities approaching 100 %.

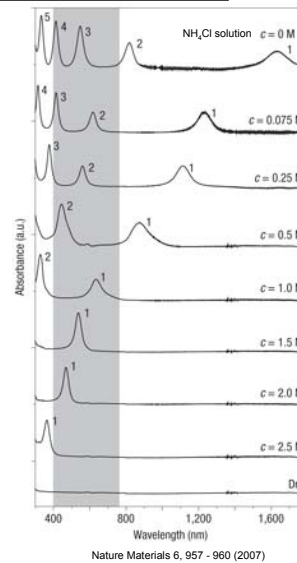
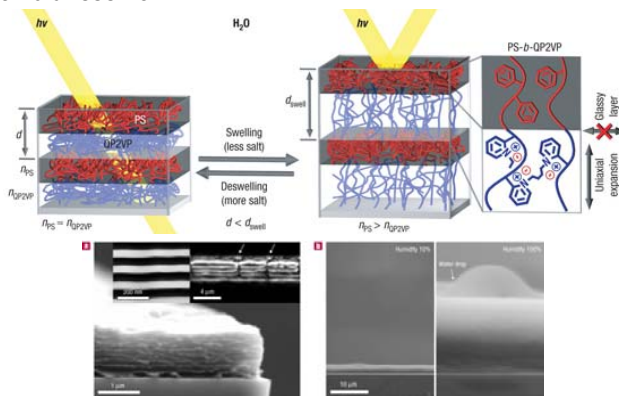
A fundamental problem encountered with co-extruded films is the occurrence of undesired thickness variations, which result in a broadening of the reflection spectrum and also unwanted higher order reflections.

Spin-coating deposition technique is also used for the preparation of multilayers.



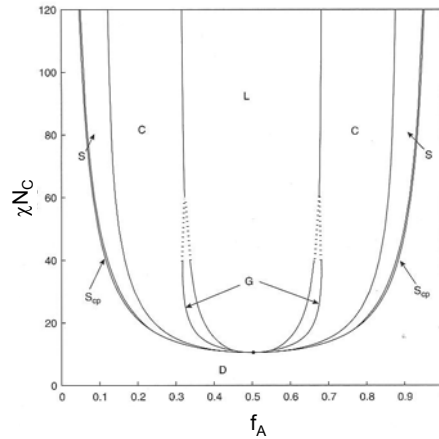
SELF-ASSEMBLED POLYMERIC MULTILAYERS

- Hydrophobic–hydrophilic polyelectrolyte block-copolymers form a simple one-dimensional periodic lamellar structure.
- This results in a responsive photonic crystal that can be tuned via swelling of the hydrophilic layers by contact with a fluid reservoir.





SELF- ASSEMBLED STRUCTURES for DIBLOCK COPOLYMERS



D = DISORDERED PHASE
L = LAMELLAE
G = GYROIDS
C = CILINDERS IN HEXAGONAL LATTICE
S = SPHERESE IN BCC LATTICE
S_{cp} = CLOSE PACKED SPHERES

- AB diblock copolymer
- Total degree of polymerization, N_c
- Flory A-B interaction parameter, χ
- Block "A" volume fraction, f_A

Microphase diagram for conformationally symmetric diblock copolymers

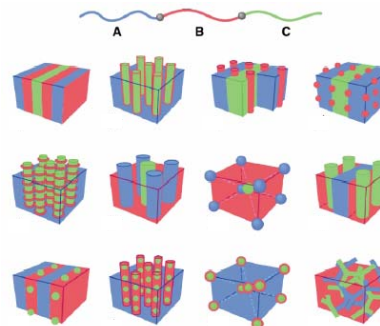


SELF- ASSEMBLED POLYMERIC STRUCTURES

DI-BLOCK

Nature of patterns	Spheres (SPH) (3D)	Cylinders (CYL) (2D)	Double gyroid (DG) (3D)	Double diamond (DD) (3D)	Lamellae (LAM) (1D)
Space group	$Im\bar{3}m$	$p6mm$	$Ia\bar{3}d$	$Pn\bar{3}m$	pm
Blue domains: A block					
Volume fraction of A block	0-21%	21-33%	33-37%	37-50%	

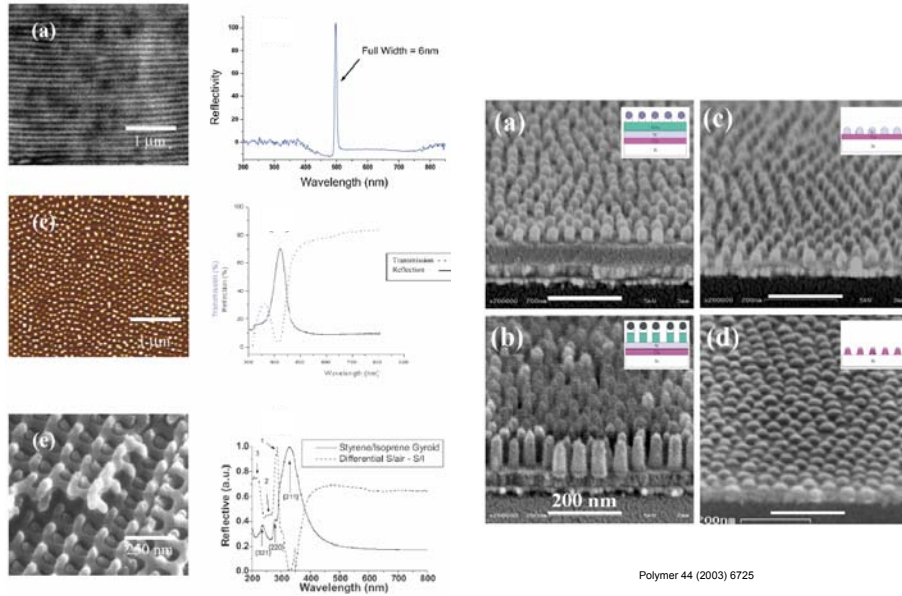
TRI-BLOCK



Schematic phase diagram showing the different classical block copolymers morphologies adopted by non crystalline di- and tri-block polymers



SELF- ASSEMBLED POLYMERIC STRUCTURES



SUMMARY

INTRODUCTION TO PHOTONIC CRYSTALS: NANOSTRUCTURED MATERIALS TO MANIPULATE LIGHT PROPAGATION & HARVESTING

- Photonic Crystals
- Natural Photonic Crystals
- Growth & Preparation of Photonic Crystals
- **Photonic Crystals Theory**
- Photonic Crystals Applications
- Photonic Crystal in Photovoltaic Devices



PHOTONIC CRYSTALS: MAXWELL'S EQUATIONS

$$\begin{aligned} \nabla \cdot \mathbf{B} &= 0 & \nabla \cdot \mathbf{D} &= 4\pi\rho & \nabla \cdot \mathbf{H}(\mathbf{r},t) &= 0 & \nabla \cdot [\varepsilon(\mathbf{r})\mathbf{E}(\mathbf{r},t)] &= 0 \\ \nabla \times \mathbf{E} + \frac{1}{c} \frac{\partial \mathbf{B}}{\partial t} &= 0 & \nabla \times \mathbf{H} - \frac{1}{c} \frac{\partial \mathbf{D}}{\partial t} &= \frac{4\pi}{c} \mathbf{j} & \nabla \times \mathbf{E}(\mathbf{r},t) + \frac{1}{c} \frac{\partial \mathbf{H}(\mathbf{r},t)}{\partial t} &= 0 \\ \rho &= 0, \mathbf{J} = 0, \mathbf{B} = \mathbf{H}, \mathbf{D} = \varepsilon \mathbf{E} & & & \nabla \times \mathbf{H}(\mathbf{r},t) - \frac{\varepsilon(\mathbf{r})}{c} \frac{\partial \mathbf{E}(\mathbf{r},t)}{\partial t} &= 0 \end{aligned}$$

$$\left. \begin{aligned} \varepsilon(\mathbf{r}) &= \varepsilon(\mathbf{r}+\mathbf{R}) & \text{Dielectric lattice} \\ \varepsilon_a, \varepsilon_b & & \text{Dielectric contrast} \end{aligned} \right\} \text{are key parameters}$$

$$\begin{aligned} \tilde{\varepsilon} &= \varepsilon + i\frac{\varepsilon}{2} \\ \varepsilon(\omega) &= \varepsilon \end{aligned} \quad \text{We assume non absorbing and non dispersive media}$$

$$\mathbf{H}(\mathbf{r},t) = \mathbf{H}(\mathbf{r})e^{i\omega t}$$

$$\mathbf{E}(\mathbf{r},t) = \mathbf{E}(\mathbf{r})e^{i\omega t}$$

Plane wave expansion



PHOTONIC CRYSTALS: MAXWELL'S EQUATIONS

$$\nabla \times \mathbf{H}(\mathbf{r},t) - \frac{\varepsilon(\mathbf{r})}{c} \frac{\partial \mathbf{E}(\mathbf{r},t)}{\partial t} = 0$$

$$\mathbf{H}(\mathbf{r},t) = \mathbf{H}(\mathbf{r})e^{i\omega t}$$

$$\nabla \times \mathbf{E}(\mathbf{r},t) + \frac{1}{c} \frac{\partial \mathbf{H}(\mathbf{r},t)}{\partial t} = 0$$

$$\mathbf{E}(\mathbf{r},t) = \mathbf{E}(\mathbf{r})e^{i\omega t}$$

non Hermitian operator

$$\hat{\mathcal{E}}\mathbf{D}(\mathbf{r}) \equiv \nabla \times \left(\nabla \times \frac{1}{\varepsilon(\mathbf{r})} \mathbf{D}(\mathbf{r}) \right) = \left(\frac{\omega}{c} \right)^2 \mathbf{D}(\mathbf{r})$$

$$\nabla \cdot \mathbf{D}(\mathbf{r}) = 0$$

$$\longrightarrow \mathbf{H}(\mathbf{r}) = \frac{i\omega}{c} \nabla \times \mathbf{D}(\mathbf{r})$$

Hermitian operator

$$\hat{\mathcal{H}}\mathbf{H}(\mathbf{r}) \equiv \nabla \times \left(\frac{1}{\varepsilon(\mathbf{r})} \nabla \times \mathbf{H}(\mathbf{r}) \right) = \left(\frac{\omega}{c} \right)^2 \mathbf{H}(\mathbf{r})$$

$$\nabla \cdot \mathbf{H}(\mathbf{r}) = 0$$

$$\longrightarrow \mathbf{E}(\mathbf{r}) = \left(\frac{-ic}{\omega\varepsilon(\mathbf{r})} \right) \nabla \times \mathbf{H}(\mathbf{r})$$

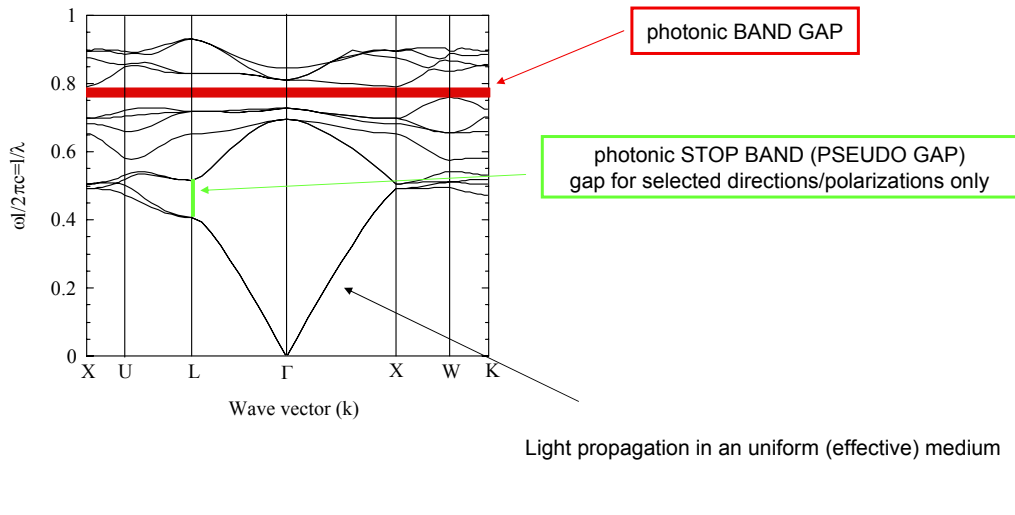
Eigenfunction

Eigenvalues
(optical modes)

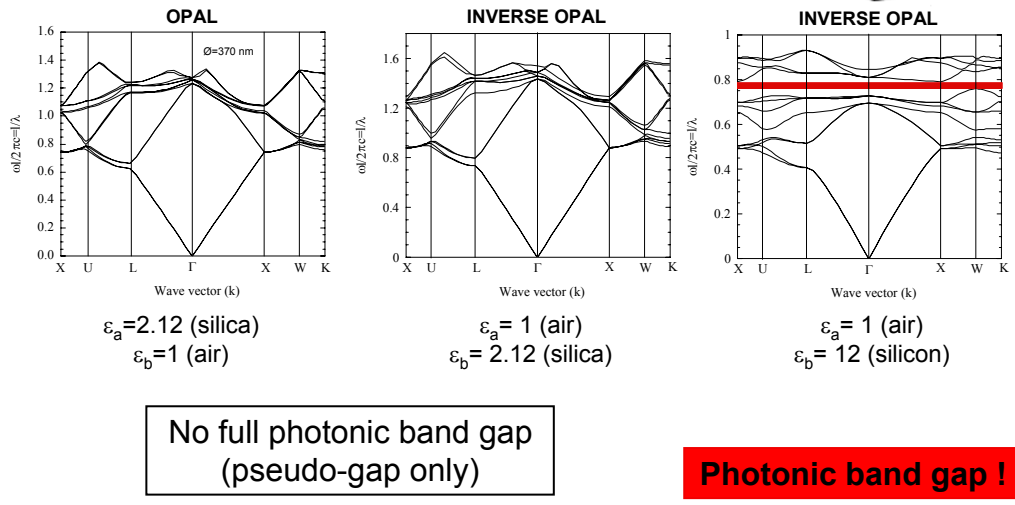
Tight mathematical similarity with Quantum Mechanics



PHOTONIC CRYSTAL: SYNTHETIC MEDIUM FOR TUNING LIGHT PROPAGATION



EFFECT OF THE STRUCTURE AND THE DIELECTRIC CONTRAST ON THE PHOTONIC BAND GAP





PHOTONIC CRYSTALS: SCALING PROPERTIES

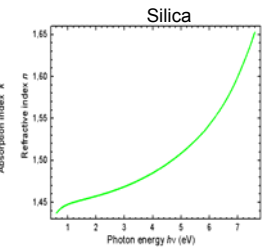
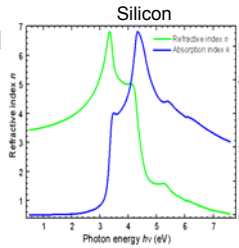


$$\mathbf{r}' = \mathbf{r} \mathbf{s}$$

$$\nabla' = \frac{\nabla}{s} \quad \varepsilon'(\mathbf{r}) = \varepsilon(\mathbf{r}/s)$$

$$s \nabla' \times \left(\frac{1}{\varepsilon(\mathbf{r}'/s)} s \nabla' \times \mathbf{H}(\mathbf{r}'/s) \right) = \left(\frac{\omega}{c} \right)^2 \mathbf{H}(\mathbf{r}'/s)$$

$$\varepsilon'(\mathbf{r}) = \varepsilon(\mathbf{r}'/s)$$



$$\varepsilon'(\mathbf{r}) = \frac{\varepsilon(\mathbf{r})}{p^2}, \quad \forall \mathbf{r}$$

$$\nabla' \times \left(\frac{1}{\varepsilon'(\mathbf{r}')} \nabla' \times \mathbf{H}(\mathbf{r}'/s) \right) = \left(\frac{\omega}{c s} \right)^2 \mathbf{H}(\mathbf{r}'/s)$$

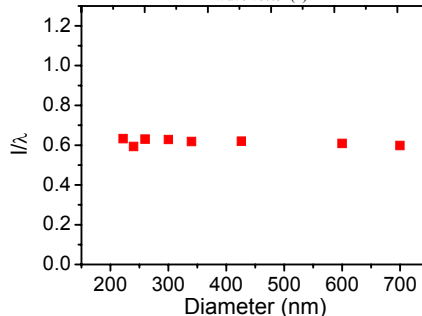
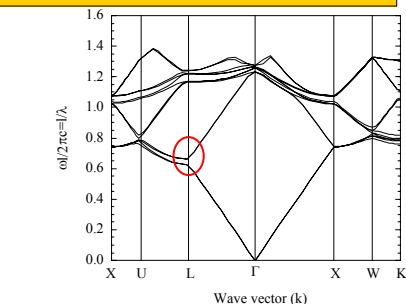
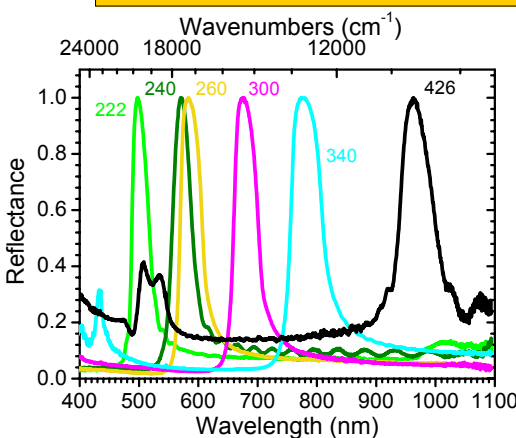
$$\nabla \times \left(\frac{1}{\varepsilon(\mathbf{r})} \nabla \times \mathbf{H}(\mathbf{r}) \right) = \left(\frac{\omega p}{c} \right)^2 \mathbf{H}(\mathbf{r})$$

$$\omega'(\mathbf{k}) = \frac{\omega(\mathbf{k})}{s}$$

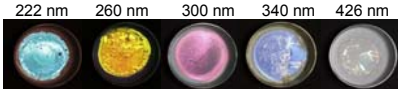
$$\omega'(\mathbf{k}) = \omega(\mathbf{k}) \cdot p$$



SCALING LAW



$$m\lambda = 2D_{111} \sqrt{n_{\text{eff}}^2 - \sin^2 \theta} \quad D_{111} = a \sqrt{\frac{2}{3}} = \frac{\ell}{\sqrt{3}}$$





QUANTUM MECHANICS AND PHOTONIC CRYSTALS: A COMPARISON...

QM in a crystal

EM in a photonic crystal

$$\hat{\mathbf{H}} \psi_{\mathbf{E}}(\mathbf{r}) \equiv \left(\frac{\mathbf{p}^2}{2m} + V(\mathbf{r}) \right) \psi_{\mathbf{E}}(\mathbf{r}) = E \psi_{\mathbf{E}}(\mathbf{r}) \quad \longleftrightarrow \quad \hat{\Theta} \mathbf{H}_{\omega}(\mathbf{r}) \equiv \nabla \times \frac{1}{\varepsilon(\mathbf{r})} \nabla \times \mathbf{H}_{\omega}(\mathbf{r}) = \frac{\omega^2}{c^2} \mathbf{H}_{\omega}(\mathbf{r})$$

The master equation is a linear Hermitian operator (Schrodinger-Maxwell)

$$V(\mathbf{r}) = V(\mathbf{r} + \mathbf{R}) \Rightarrow \Psi_{\mathbf{k}}(\mathbf{r}) = u_{\mathbf{k}}(\mathbf{r}) e^{i\mathbf{k} \cdot \mathbf{r}} \quad \longleftrightarrow \quad \varepsilon(\mathbf{r}) = \varepsilon(\mathbf{r} + \mathbf{R}) \Rightarrow \mathbf{H}_{\mathbf{k}}(\mathbf{r}) = u_{\mathbf{k}}(\mathbf{r}) e^{i\mathbf{k} \cdot \mathbf{r}}$$

Periodicity of the system (potential-dielectric constant)

$$\psi(\mathbf{r}, t) = \sum_{\mathbf{E}} c_{\mathbf{E}} \psi_{\mathbf{E}}(\mathbf{r}) e^{i\mathbf{E}t/\hbar} \quad \longleftrightarrow \quad \mathbf{H}(\mathbf{r}, t) = \sum_{\omega} c_{\omega} \mathbf{H}_{\omega}(\mathbf{r}) e^{i\omega t/\hbar}$$

Main function containing all the information (normalizable - normalizable & transverse)

$\int |\psi(\mathbf{r}, t)|^2 d\mathbf{r} = 1$ $\nabla \cdot \mathbf{H} = 0$



QUANTUM MECHANICS AND PHOTONIC CRYSTALS: A COMPARISON...

QM in a crystal

EM in a photonic crystal

Electron-electron repulsive interaction
Large scale computation difficult

In the linear regime, light modes can pass right through one another undisturbed and can be calculated independently

$$E_{\text{var}} = \frac{\langle \psi | \hat{\mathbf{H}} | \psi \rangle}{\langle \psi | \psi \rangle}$$

$$E_{\text{var}} = \frac{(\mathbf{H}, \hat{\Theta} \mathbf{H})}{(\mathbf{H}, \mathbf{H})}$$

Eigenstates with different energies are orthogonal, they have real eigenvalues, and can be found with a variational principle

Modes with different frequencies are orthogonal, they have real positive eigenvalues, and can be found with a variational principle

E_{var} is minimized when ψ is an eigenstate of \mathbf{H}

E_{var} is minimized when \mathbf{H} is normal mode of Θ

The wavefunction concentrates in regions of low potential, while remaining orthogonal to lower states

The fields concentrates their electrical energy in high- ε regions, while remaining orthogonal to lower modes



QUANTUM MECHANICS AND PHOTONIC CRYSTALS: A COMPARISON...

QM in a crystal

The eigenvalue E of the Hamiltonian

System energy

The natural scale of the system is provided by the Bohr radius

Scale length of the system

The band structure $E_n(\mathbf{k})$ tells us the energies of the allowed eigenstates.

The electron wave scatters coherently from the different potential regions

Band structure and gap

Inside the **electronic gap** no propagating electrons are allowed to exist

The band above the gap is the conduction band; the band below the gap is the valence band

EM in a photonic crystal

The electromagnetic energy

$$E = \frac{1}{8\pi} \int d\mathbf{r} \left(\frac{1}{\epsilon} |\mathbf{D}|^2 + |\mathbf{H}|^2 \right)$$

There is not a natural scale: the solutions are scalable to any length

The functions $\omega_n(\mathbf{k})$ tell us the frequencies of the allowed harmonic modes.

The electromagnetic fields scatter coherently at the interface between different dielectric regions

Inside the **photonic band gap** no modes are allowed to exist

The band above the gap is the **air band**; the band below the gap is the **dielectric band**



QUANTUM MECHANICS AND PHOTONIC CRYSTALS: A COMPARISON...

QM in a crystal

A defect (foreign atom in a crystal) breaks the translational symmetry of the atomic potential and it might create an allowed state in the **electronic band gap**, thereby allowing a localized electronic state around the defect.

Defect engineering

Donor atoms pull states from the conduction band into the gap; acceptor atoms pull states from the valence band into the gap

EM in a photonic crystal

A defect changing ϵ in a certain region (point, line, plane) breaks the translational symmetry of $\epsilon(\mathbf{r})$ and it might create an allowed state in the **photonic band gap**, thereby permitting a localized mode around the defect.

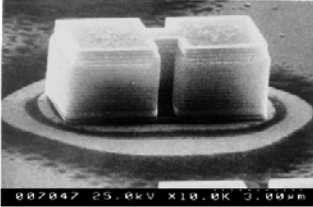
Dielectric defects pull states from the “**air**” band into the gap; “**air**” defects pull states from the **dielectric** band into the gap

We can tailor the **electronic** properties of materials to our needs

We can tailor the **optical** properties of materials to our needs



OPTICAL MODES IN PHOTONIC MOLECULES

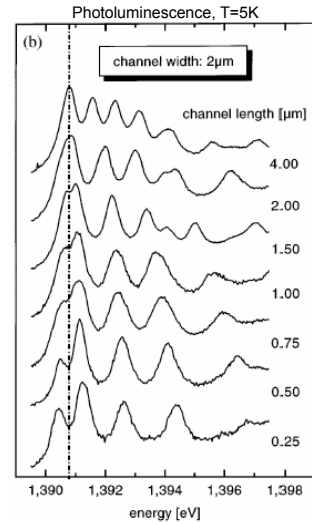


A GaAs layer was surrounded by highly reflecting GaAsAlAs Bragg mirrors. A 7 nm wide $\text{In}_{0.14}\text{Ga}_{0.86}\text{As}$ quantum well was placed in the center of the GaAs cavity. Photonic molecules were prepared by lithographic patterning of this cavity.

Photonic Molecules

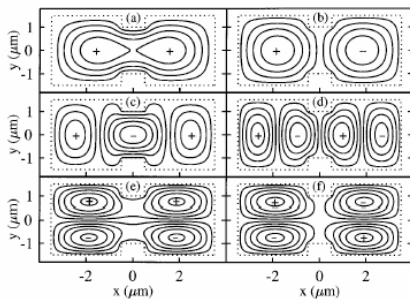
Coupled optical microcavities (similarity between the field eigenmodes and the electronic structure of real molecules)

In contrast with waveguides in a PhC (line defects) where a broad range of frequencies are allowed to propagate within the bandgap, photonic molecules structure allows transmission only at cavity resonance frequencies

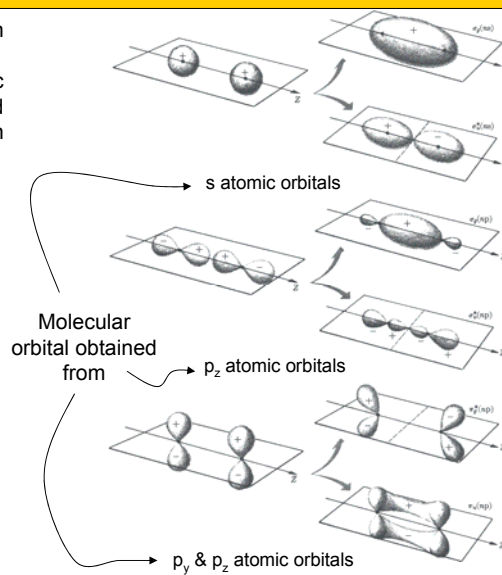


ANALOGIES BETWEEN MOLECULES AND PHOTONIC MOLECULES

- In molecules the bonding strength depends on Coulomb forces between nuclei and electrons
- The interaction of photon modes in photonic molecules is determined by the geometry and then can be varied by structure design (length or width of the interconnecting channel)



Calculated electric field distributions of the six lowest confined optical modes in photonic molecules.





ELECTROMAGNETIC VARIATIONAL THEOREM: AIR & DIELECTRIC BANDS

- Unlike electrons in a semiconductor which are constrained by Fermi statistics and therefore have to be excited from the valence band to the conduction band to become mobile, photons are bosons which propagate freely at frequencies both above and below the PBG.
- Thus the terms 'valence band' and 'conduction band' may not be appropriate in the context of a PhC.
- Instead, bands above and below a PBG can be distinguished by applying the electromagnetic variational theorem:

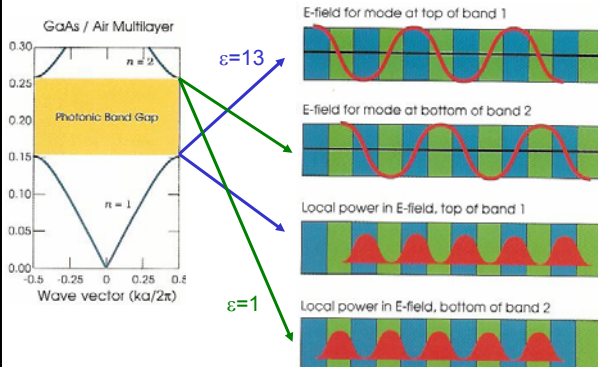
$$E_f(H) = \frac{1}{2} \frac{\left(\frac{\hat{H}, \hat{\Theta}H}{(H, H)} \right)}{\left(\frac{H, H}{2(H, H)} \right)} = \left(\frac{1}{2(H, H)} \right) \int dr \frac{1}{\epsilon} |\nabla \times H|^2 = \left(\frac{1}{2(H, H)} \right) \int dr \frac{1}{\epsilon} \left| \frac{\omega}{c} D \right|^2 \quad (F, G) \equiv \int dr F^*(r) \cdot G(r)$$

- According to this theorem, for modes in the **lower photonic band**, the power of modes lies primarily in the **high-index regions**, whereas for modes in the **upper photonic band** the power lies in the **low-index regions**. In PCs, the low-index regions are often air regions. For this reason it is more meaningful to refer to the **band above a PBG as the 'air' band**, and the one **below the gap as the 'dielectric' band**.



ELECTROMAGNETIC VARIATIONAL THEOREM: LIGHT LOCALIZATION

- Standing waves in the PC can be with the NODE in the high or low ϵ material (any other position would violate the symmetry of the unit cell about its center).
- Low frequency modes concentrate their energy in the **high ϵ material** while high frequency modes concentrate their energy in **low ϵ material**
- At the edges of the photonic band gap the field is localized in different composing material



- A frequency difference exists between the two cases.

- The mode just **under the gap** has its power concentrated in the **high ϵ material** giving it a **lower frequency**.

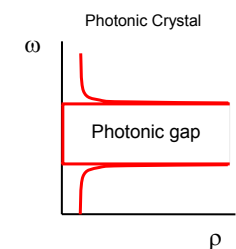
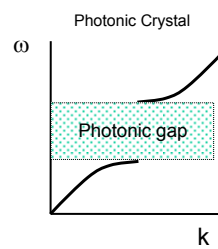
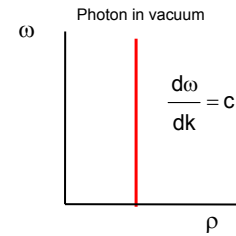
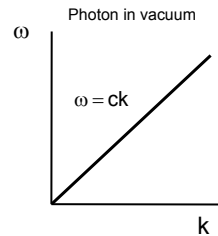
- The mode just **above the gap** has most of its power in **low ϵ regions** so its **frequency is raised**.

- This explains in a different way the **physical origin of the photonic band gap**.

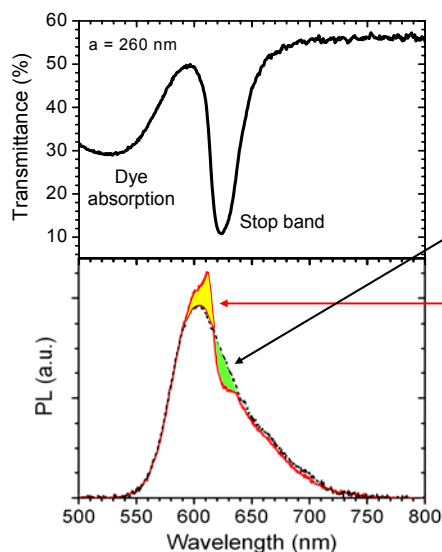


LIGHT LOCALIZATION

- Photons in the void possess a linear dispersion, which provides a constant density of photonic state (DOS).
- Due to their peculiar photonic band structure, PhCs modify the DOS of the void.
- At the band gap, the DOS is reduced thus preventing the light to propagate.
- At the band gap edges, bands are flat and then the DOS shows a divergence.
- Since at the band gap edges the group velocity of light is $v_g = d\omega/dk = 0$, there light-matter interaction is expected to increase.
- At the edges field localization also occurs.
- These effects have been used to enhance emission from dyes embedded inside the PhC.



PL DIRECTIONAL ENHANCEMENT @ BAND EDGE



• Light emission is inhibited due to the reduced mode density within the Stop Band

• PL enhancement is observed at the high-energy edge of the Stop Band where localization occurs in the low ϵ material (solution)



SUMMARY

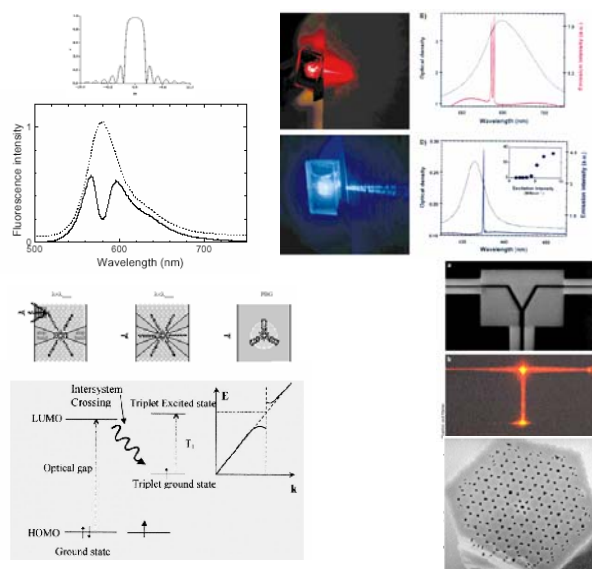
INTRODUCTION TO PHOTONIC CRYSTALS: NANOSTRUCTURED MATERIALS TO MANIPULATE LIGHT PROPAGATION & HARVESTING

- Photonic Crystals
- Natural Photonic Crystals
- Growth & Preparation of Photonic Crystals
- Photonic Crystals Theory
- **Photonic Crystals Applications**
- Photonic Crystal in Photovoltaic Devices



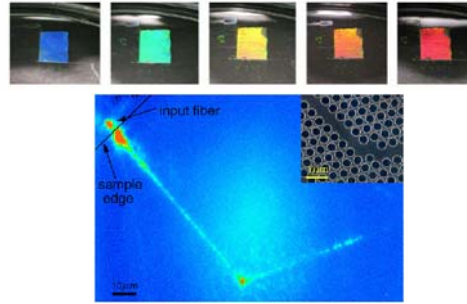
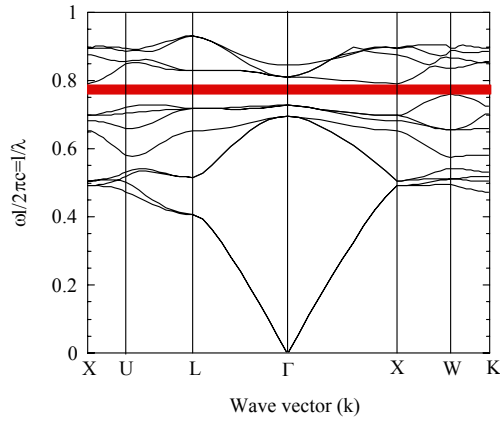
WORKING PHOTONIC CRYSTALS

- Bragg reflectors and microcavities (dielectric mirrors)
- Inhibition of spontaneous emission inside the photonic cavity
- Thresholdless laser
- Defects acting as waveguides
- Light localization
- e-h recombination quenching in transistors and solar-cells
- Optical switching
- Sensors



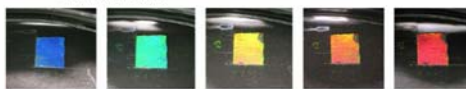
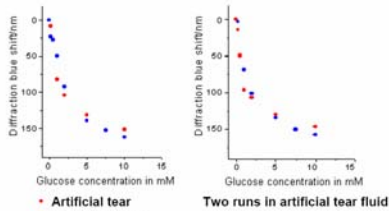
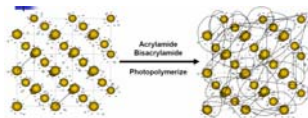


PHOTONIC CRYSTAL: SYNTHETIC MEDIUM FOR TUNING LIGHT PROPAGATION



SENSING BY PHOTONIC CRYSTALS

Colloidal Crystals Arrays

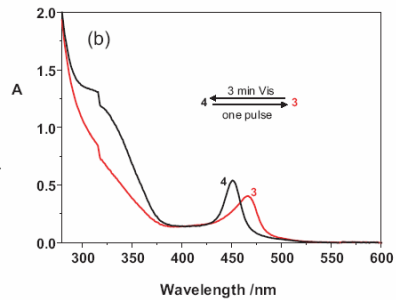
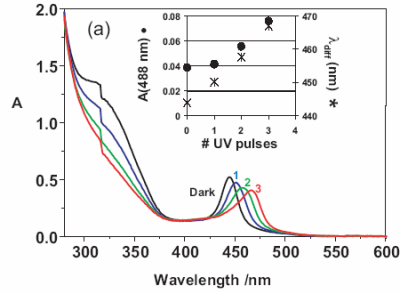
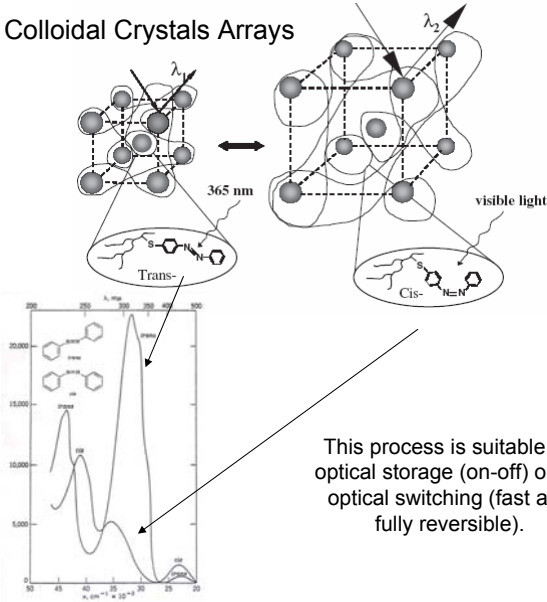


CCAs have been also used for sensing ammonia, Pb^{2+} , nerve agents, creatinine...



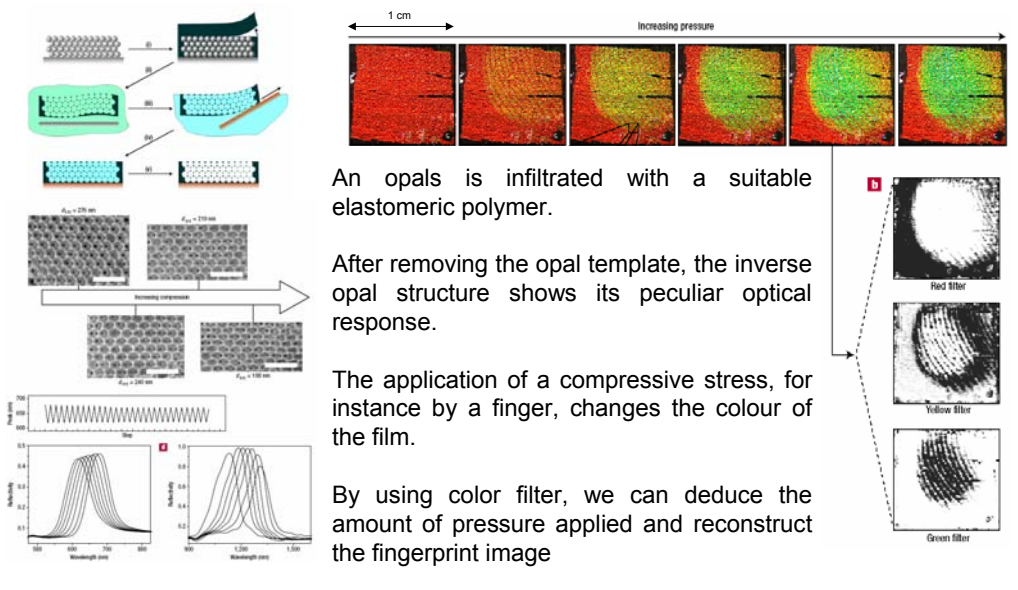
PHOTONIC CRYSTALS OPTICAL MEMORIES

Colloidal Crystals Arrays



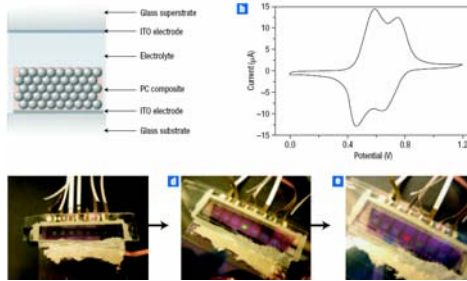
COLOUR FINGERPRINTING BY ELASTIC PhC

A.C. Arsenault et al. Nat. Mater. 5, 179 (2006)





PhC FULL-COLOR PAPER-LIKE DISPLAYS

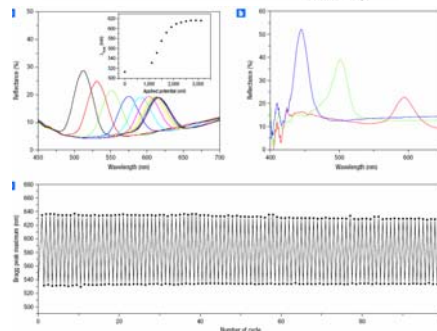


A.C. Arsenault et al. Nature Photonics 1, 468 (07)

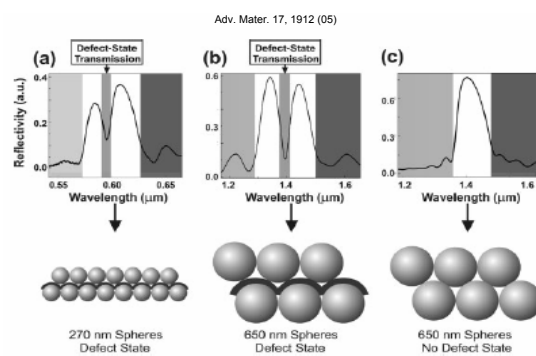


Decreasing crosslink density

- A silica opal is infiltrated with a crosslinked network of an iron-based metallopolymer (polyferrocenylsilane).
- Electrical actuation is achieved by an incorporated sealed thin-layer electrochemical cell.
- A change of the applied potential modify the PhC structure thus inducing a color change.
- Color tunability is achieved by structural changes thus reducing bleaching problems typical of molecular dyes.
- Very good reproducibility is obtained.
- This technology can be used as a photonic ink suitable for paper-like displays.



“DEFECTS” IN PHOTONIC CRYSTALS

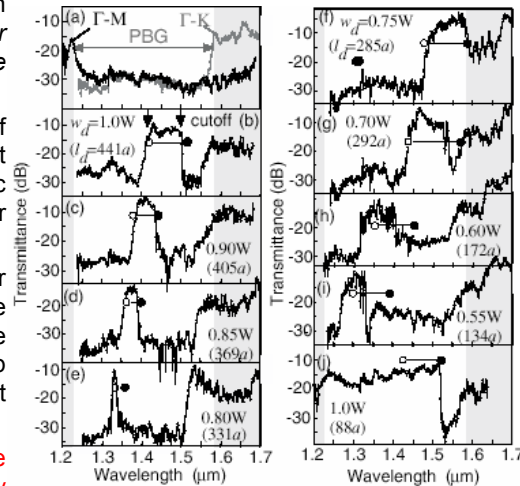


Structural/dielectric defects generate gap states (allowed modes within the photonic band gap)

Electromagnetic fields cannot propagate @ stop band, but defects relax this constraint inducing light confinement

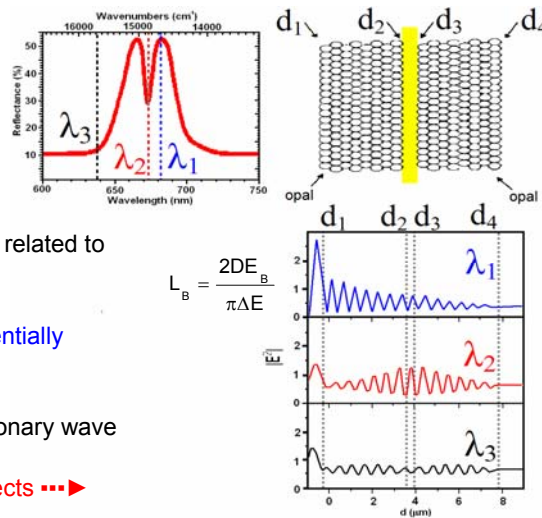
“DEFECTS” IN PHOTONIC CRYSTALS

- The frequency of a defect mode is an *increasing function of the volume of an air defect and a decreasing function of the volume of a dielectric defect.*
- For air defect, the larger the volume of material removed, the further the defect mode is pushed from the lower photonic band edge into the gap (that is, the higher the frequency of the defect mode).
- Conversely, for a dielectric defect, the larger the volume of high-index material added, the further the defect mode is pushed from the upper photonic band edge into the band gap (that is, the lower the frequency of the defect mode).
- Thus the frequency of a defect mode can be ‘tuned’ to any desired value within the gap by adding (or removing) the appropriate amount of dielectric material from a unit cell.



Transmission spectra (TE polarization) of defect-free 2D-PhC, and line defects of different widths (W)

DEFECT ENGINEERING

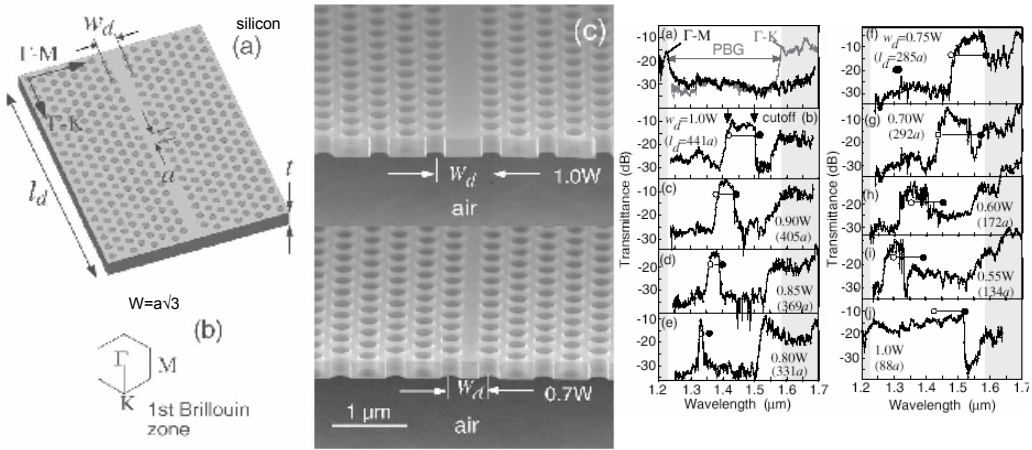


The importance of structural defects is related to light localization effects

- λ_1 (stop band), light intensity is exponentially attenuated
- λ_3 (stop band edge), light forms a stationary wave
- λ_2 (defect), light is localized within defects \rightarrow threshold lowering for lasing or NLO

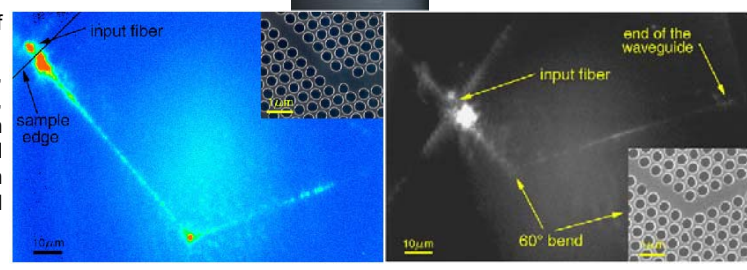
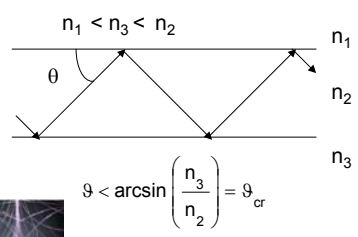
$$L_B = \frac{2DE_B}{\pi\Delta E}$$

PHOTONIC CRYSTAL WAVEGUIDES



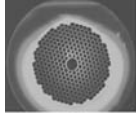
PHOTONIC CRYSTAL vs STANDARD WAVEGUIDES

- In standard waveguides, light confinement is achieved through total internal reflection.
- The difficulty of guiding light **around tight bends** has limited the development of small-scale interconnections. In conventional fiber-optic waveguides, a **tight curve results in an angle of incidence that is too large for total internal reflection to occur. Light escapes at the corners** weakening the signals. Photonic-crystal waveguides can confine light in a narrow beam around tight corners.
- A key advantage of photonic-crystal waveguides is their size, about **100x100 μm²**, compared with conventional arrayed waveguide gratings, which are roughly **4 cm long and 1 to 2 cm wide**.



PHOTONIC CRYSTAL OPTICAL FIBERS

Only constructive scattering from a photonic bandgap structure can guide light down hollow-core fibers (facing left)

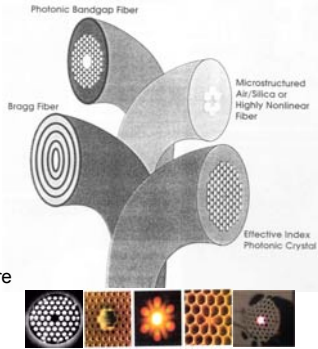


high-power laser signals could potentially be transmitted along the fibre without damaging

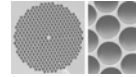
Whenever there is silica or air in the core, photonic crystal fibers could take the ability of optical fiber to the extreme

OmniGuide Communications claims expected loss for Bragg fibers: 0.01dB/Km and 10⁴ reduction of the non linear effects (conventional silica fiber 0.2 dB/ Km).

Hollow core fibers show reduced Rayleigh scattering effects but other processes dominated over it, like leakages from the core. Measured losses are 0.3 dB/m.



Other photonic crystal fibers use a modified form of total internal reflection to guide light along silica core (facing right)



- A drawback with conventional optical fibres is that different wavelengths of light can travel through the material at different speeds (dispersion).
- Over long distances, time delays occurs between signals that are encoded at different wavelengths.
- Then a light pulse travelling through such a fibre broadens out, thereby limiting the amount of data that can be sent.
- The "holey" fibre has a regular lattice of air cores running along its length and transmits a wide range of wavelengths without suffering from dispersion.

THRESHOLDLESS LASER

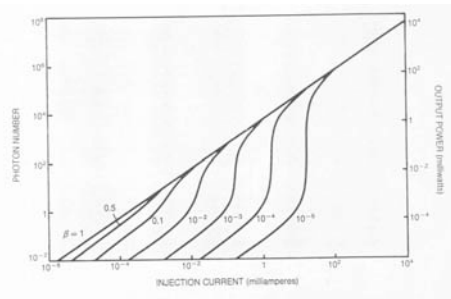
LASING THRESHOLD

- Active medium gain
- Cavity parameters
- Losses
- Gain volume



A. Sherer et al. Science 284, 1819(99)

$$\beta = \frac{\text{number of photons emitted in the laser mode}}{\text{total number of emitted photons}}$$

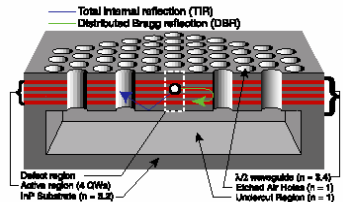


$\beta=10^{-5}$ in semiconducting lasers

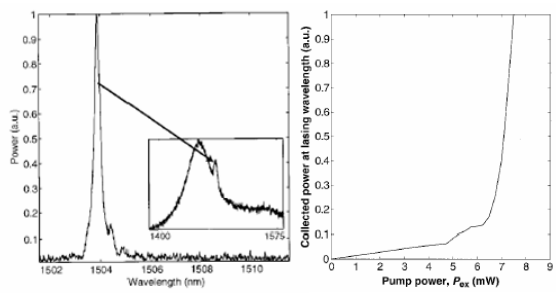
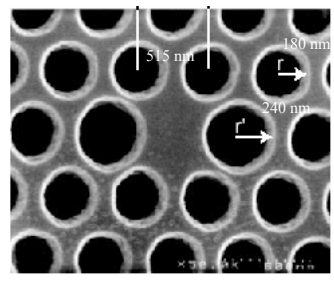
$\beta=10^{-1}$ in microcavities



2D PBG DEFECT MODE LASER



4 Strained InGaAsP Quantum Wells in InP bulk
 $\beta=0.65$, $Q=250$



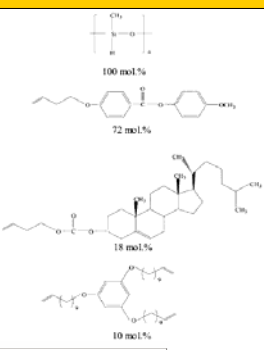
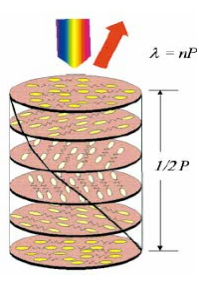
STILL LIMITING FACTORS:

- Low Q
- Poor thermal heat-sinking
- Inefficient optical pumping

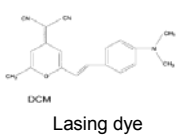
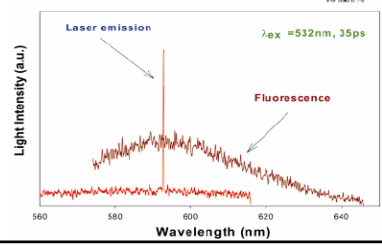
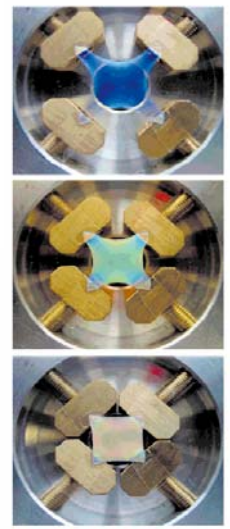
A. Sherer et al. Science 284,1819 (99)



TUNABLE MIRRORLESS LASING IN CHOLESTERIC LIQUID CRYSTAL ELASTOMERS



Poly[oxy(methylsilylene)]
Achiral nematogenic monomer
Chiral cholesterilcarbonate
Cross-linking agent

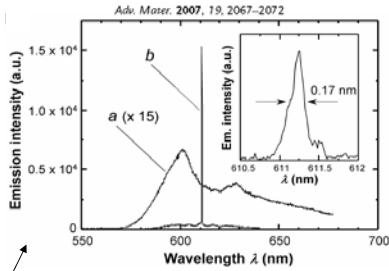
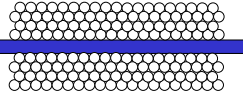


Adv. Mater. (2001) 13, 1069

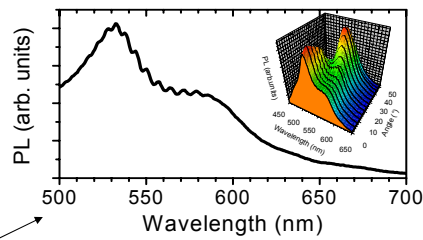
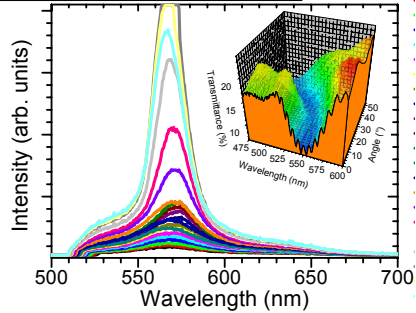


DEFECT@OPAL: ASE & LASING

Active layer (conjugated molecule or polymer)



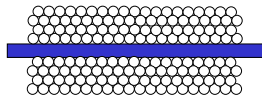
- Lasing inside the stop band
- No defect modes are reported
- In opal sandwich structures, ASE is achieved & defect modes are clearly observed



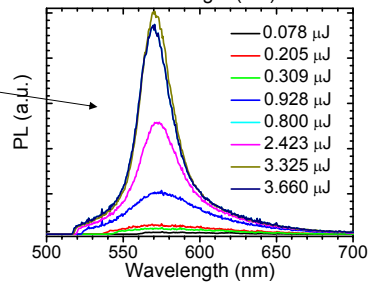
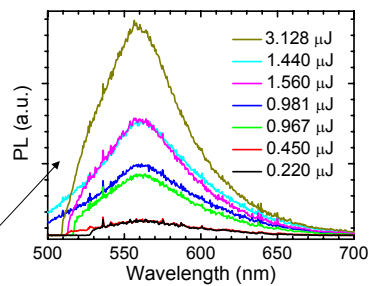
PCCP 11, 11515 (09)



DEFECT@OPAL: ASE & PHOTOBLEACHING



- For free-standing polymer film, no ASE is observed upon increasing fluence.
- For plane defect @ opal, ASE is observed upon increasing pumping fluence.
- Photobleaching prevents to achieve the lasing threshold

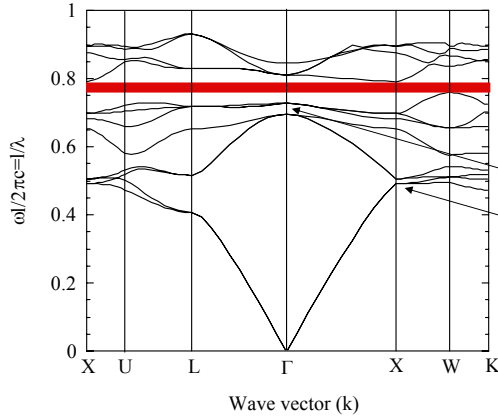


PCCP 11, 11515 (09)



PHOTONIC CRYSTAL: SYNTHETIC MEDIUM FOR TUNING LIGHT PROPAGATION

Zero group-velocity $d\omega/dk=0$: distributed feedback (DFB) lasers



Flat bands, $d\omega/dk=v_g \rightarrow 0$
slow light, light localization, inhibition
of spontaneous emission... (NLO
effects, lasing)



PHOTONIC CRYSTAL: LASING

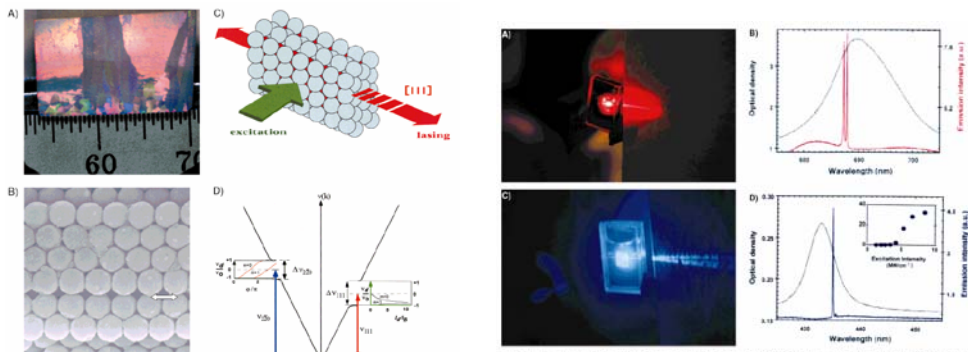


Fig. 1. A) Photograph of the polycrystalline opal sample that was cut to provide the investigated single crystal slabs. The illumination provides homogeneous diffraction-band coloration due to single crystals. B) SEM image in the [111] direction for a single crystal opal showing regions separated by a stacking fault on a {111} plane. The double-headed arrow (200 nm long) is parallel to this stacking fault (which is not orthogonal to the image plane). C) Schematic representation of the experimental geometry used for measuring laser action in the [111] direction for a double-headed opal slab with stripe excitation along the opal [111] direction. D) Schematic photonic dispersion relations along the [111] and [220] directions in an opal photonic crystal, showing non-overlapping photonic bandgaps in the red and blue spectral ranges. The dependence of n on the direction length, k , for $n = 1.45$ (red) and 1.54 (blue) is schematically shown in the [111] bandgap, and the dependence of n on phase shift k for $k_x/k_y/k_z$ (for $n=1.5$ and 1) is shown inside the [220] bandgap.

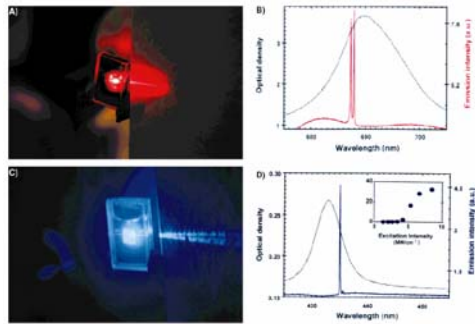


Fig. 2. Laser action from an opal single crystal adulterated with different dyes in a quartz cavity. A) Red laser emission along the [111] opal growth direction, the dye solution is 10^{-4} M rhodamine in methanol. B) The [111] opal laser emission spectrum (solid curve), showing two AlGaAs-referenced DFB laser lines inside the [111] stop band, superimposed on the regular photoluminescence background (which is perfectly suppressed inside the stop band). Excitation was at three times the threshold intensity of 100 mW/cm². The optical density spectrum of the opal slab near the [111] stop band (dashed curve) is shown for comparison. C) Violet laser emission along the [220] opal direction for a dye solution comprising a 10^{-4} M solution of methanol and benzoin alcohol. D) The [220] laser emission spectrum (solid curve) showing a single laser line (and a weak satellite) inside the [220] stop band superimposed on the regular photoluminescence background. Excitation was at three times the threshold light intensity of 100 mW/cm². The opal optical density spectrum near the [220] stop band (dashed curve) is shown for comparison. The inset shows the dependence of laser output intensity on excitation intensity.

- Tunable lasing emission in 3D switchable directions
- Lasing is due to gap-state (defects) with polarization 15:1
- Different types of wavelength tunability are possible [change of resonance for different crystalline plane (230 nm), change of n_{eff} (70 nm), slight change of stripe direction (6 nm)]
- Many independent laser cavities existing in a photonic crystal are observed by simultaneously lasing in various colors and directions



PHOTONIC CRYSTAL: RANDOM LASING

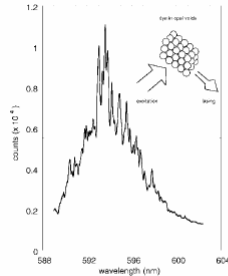


Fig. 4. Random laser emission spectrum of a DOO-PPV in toluene solution that is infiltrated into an opal photonic crystal. The inset shows the opal, which is composed of silica spheres in a closed packed lattice, and the laser excitation and collection geometries.



Adv. Mater. 13, 760 (2001)

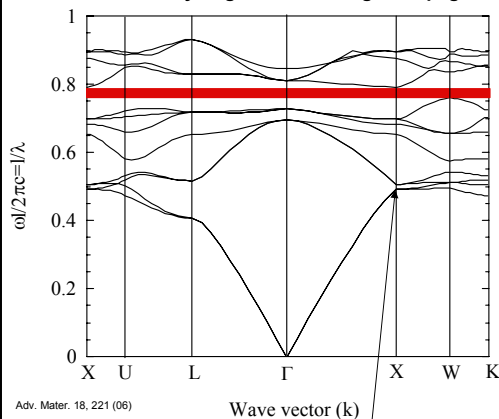
Fig. 5. The laser beams of two simultaneous random lasers in an infiltrated opal photonic crystal. The two dyes, Oxazine 670 (red) and Stilbene 140 (blue) were dissolved in methanol solution that was infiltrated into the opal. The red emission was excited at 532 nm, whereas the blue emission was excited at 355 nm using a pulsed Nd:YAG laser.

- Random lasing is a generic phenomenon that occurs in disordered media at excitation intensity regime higher than that giving rise to ASE.
- The emitted radiation is coherent and its spectrum contains many laser modes from which a typical cavity length can be obtained (polarization 1.5:1)
- Since random cavities are independent each other, laser emission in several colors is possible when mixing different dyes
- This lasing action occurs well above threshold and is unrelated to the photonic stop band, but overlapped to the dye maximum emission spectrum



PHOTONIC CRYSTAL: SUPER PRISM EFFECT

Extraordinary Angle-Sensitive Light Propagation



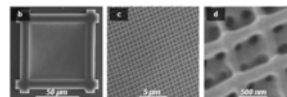
Adv. Mater. 18, 221 (06)

strong curvature (non linear dispersion):
super-prisms

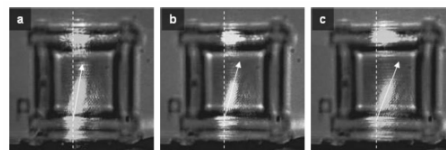
More than 10° variation of the angle by changing λ from 1000 to 1010 and then to 1020 nm

Due to band structure anisotropy, extraordinary angle-sensitive propagation of light inside a PhC can be achieved at different wavelengths.

This effect, called SUPERPRISM phenomenon, is observed at high frequencies where anisotropy is strong and negative refraction and birefringence are expected



Two-photon induced polymerization

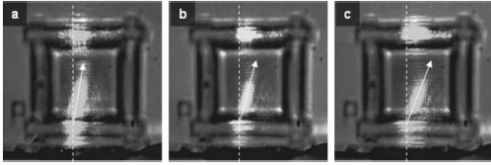


4° fixed incidence angle

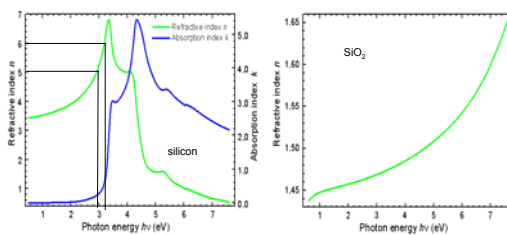


PHOTONIC CRYSTAL: SUPER PRISM EFFECT

Adv. Mater. 18, 221 (06) **4° fixed incidence angle**



More than 10° variation of the angle by changing λ from 1000 to 1010 and then to 1020 nm



$$\delta n_{\text{Si}}(3 \text{ eV}) = 1 \rightarrow \delta \lambda = 83 \text{ nm}$$

$$n_i \sin \theta_i = n_t \sin \theta_t$$

$$\theta_i = 4^\circ, n_i = 1, \delta \theta = 10^\circ$$

$$n_t(1020) = n_t(1000) + \delta n$$

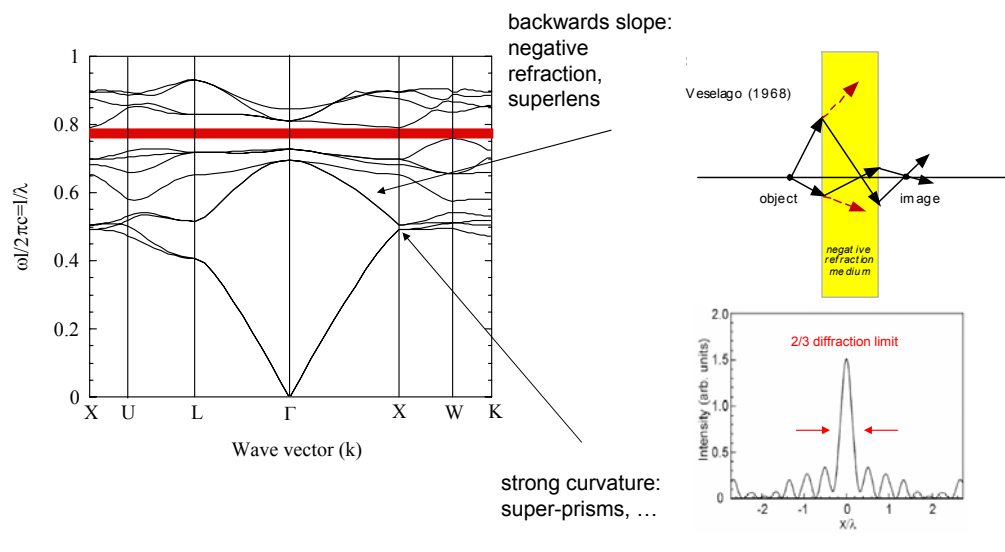
Assuming $n_t = 1.3$, from Snell's law $\theta_t = 3^\circ$

$$\delta n = n_i \sin \theta_i \left(\frac{1}{\sin \theta_t} - \frac{1}{\sin(\theta_t + \delta \theta)} \right) = 1.02$$

In a standard TRANSPARENT material, a similar variation of the refracted angle (10°) over 20 nm, would be assigned to a REFRACTIVE INDEX INCREASE OF 1!!!!



PHOTONIC CRYSTAL: SUPERPRISM & NEGATIVE REFRACTION





PHOTONIC CRYSTAL: SUPERPRISM & NEGATIVE REFRACTION

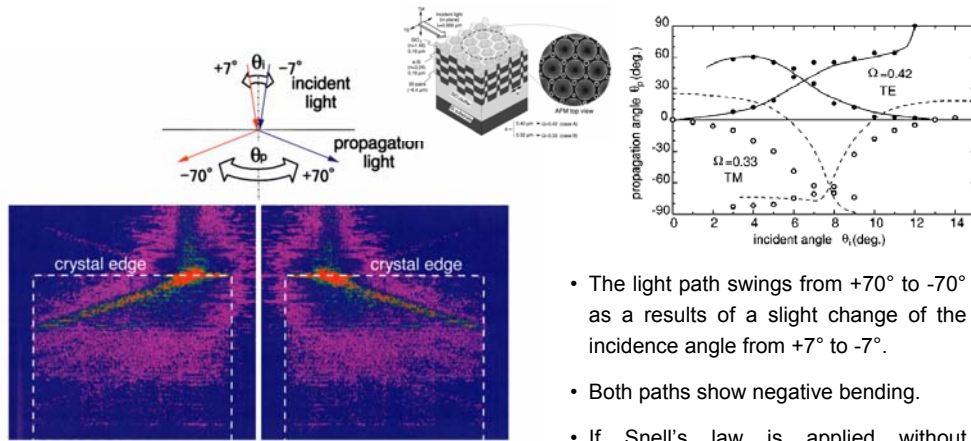


FIG. 1. (Color) Photographs showing light-beam swing inside the photonic crystal. The tilting angle of the incident light was slightly altered from $+7^\circ$ (left) to -7° (right). Both paths show negative bending. The incident light has a wavelength corresponding to the normalized frequency $\Omega = 0.33$ (defined later) with the TM polarization. The angles were measured from normal to the crystal edge ($T \rightarrow M$ crystal direction). The crystal size is $500 \mu\text{m} \times 500 \mu\text{m}$.

Kosaka, *PRB* 58, R10096 (1998)

Appl. Phys. Lett. 81, 2352 (2002)

- The light path swings from $+70^\circ$ to -70° as a result of a slight change of the incidence angle from $+7^\circ$ to -7° .
- Both paths show negative bending.
- If Snell's law is applied without regard to photonic band anisotropy, this phenomenon implies a **negative refractive index**



SUMMARY

INTRODUCTION TO PHOTONIC CRYSTALS: NANOSTRUCTURED MATERIALS TO MANIPULATE LIGHT PROPAGATION & HARVESTING

- Photonic Crystals
- Natural Photonic Crystals
- Growth & Preparation of Photonic Crystals
- Photonic Crystals Theory
- Photonic Crystals Applications
- Photonic Crystal in Photovoltaic Devices



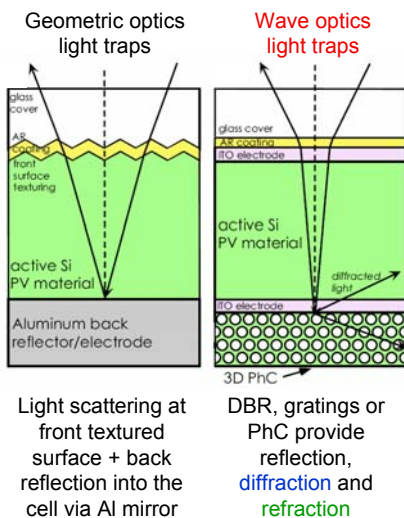
PHOTONIC CRYSTAL IN PHOTOVOLTAIC DEVICES

- Photonic Crystal in Photovoltaic Devices
 - 1) c-Silicon PV Cells
 - 2) Polymeric Bulk Heterojunctions
 - 3) Fluorescent Concentrators
 - 4) DSSC (3D & 1D PhC)



PhC in PHOTOVOLTAIC CELLS: c-Si

c-Si solar cell



Light scattering at front textured surface + back reflection into the cell via Al mirror

DBR, gratings or PhC provide reflection, diffraction and refraction

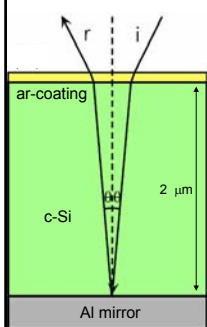
Advantages of wave optics based structures:

- **Reflection superior to aluminum mirrors.**
DBR with high index contrast and PhC can reflect light over a broad range of incident angles and wavelengths since corresponding propagating modes are wholly forbidden.
No metal required (no absorption, no charge recombination).
- **Incoming beams are diffracted into highly oblique angles, according to Bragg's law.**
Diffraction improves light trapping by increasing the distance that light must travel to return to the front surface of the cell (optical depth).
If the angle of the diffracted beam is greater than the critical angle, it will also be internally reflected back into the solar cell.
- **Frequencies outside the photonic band gap can be refracted into modes with a high photon DOS in order to improve absorption efficiency.**
Coupling can take place via a superprism-type effect. All of these effects increase the time spent by photons inside the solar cell, which helps to maximize the absorption probability.

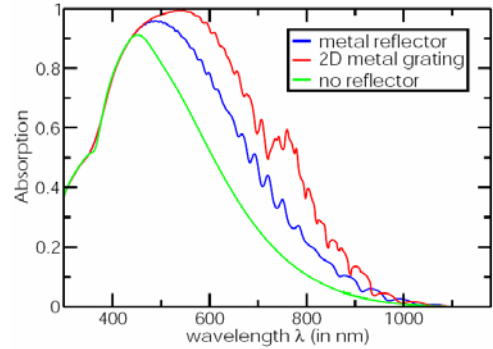
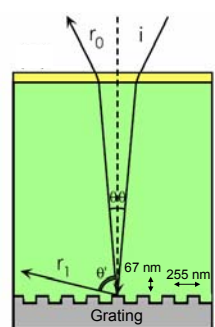
These wave optics-based approaches offer the advantage of lower materials usage (reduced thickness) as well as lower bulk recombination losses and potentially higher open-circuit voltages (increased light intensity inside the cell).

PhC in PHOTOVOLTAIC CELLS: c-Si

Geometric optics
light traps



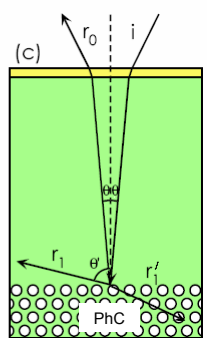
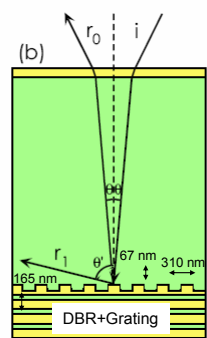
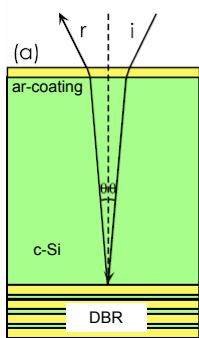
Wave optics
light traps



First-order diffraction
(threshold 920 nm for c-Si)
Profile shape, incident
angle, volume fraction, etch
depth ... can be optimized

The ability of the PV cell to absorb photons is enhanced when a metal grating is added.
(No recombination losses at metal surface are taken into account)

PhC in PHOTOVOLTAIC CELLS: c-Si



c-Si $n \approx 3.5$
SiO₂ $n \approx 1.5$

- Improved PV cell efficiency is obtained for all wave optics structures.
- Careful design is needed.
- Cell production ?

Wave optics structure	PV Cell efficiency (%)
Al reflector ^{+,*}	12.72 (13.77)
Al grating ^{+,*}	(17.88 1D-19.29 2D)
DBR (8 periods)	12.44
DBR+1D grating	15.42 (+24%)
DBR+2D grating	16.32 (+31%)
Triangular PhC	15.79 (+27%)
Woodpile PhC	15.42 (+24%)
Inverse opal PhC	15.73 (+26%)

^{*} Recombination losses at metal surface are NOT taken into account
^{*} Data neglecting absorption losses are in parenthesis



PhC in PV CELLS: BULK HETERO JUNCTION

OPV efficiency depends three length scales: absorption penetration depth ($1/\alpha \sim 100 \text{ nm} - 1 \mu\text{m}$), exciton diffusion length ($\sim 10 \text{ nm}$), and carrier diffusion length (strongly dependent on supramolecular order).

BHJ cells have active layer thicknesses of $\sim 100 \text{ nm}$ which is a reasonable trade-off between optical absorption and reduced mobility.

This thickness is adequate to absorb most photons in the visible range due to the strong extinction coefficient of organic materials.

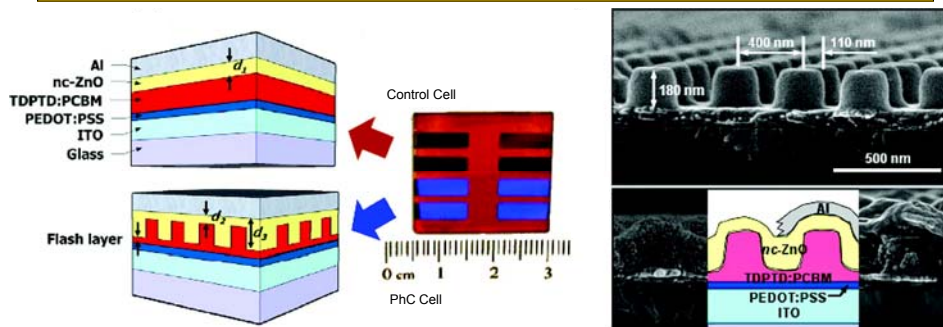
However, the sun's maximum photon flux is located around 700 nm , near the band edge of many BHJ materials where absorption is weak. In this case, reduced light absorption is expected.

Even though electronic state engineering via custom synthesis has produced low-bandgap polymers, their broad and weak absorption tails in the NIR require much larger thickness thus reducing cell performances due to carrier mobility limitations.

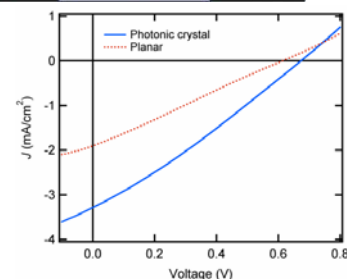
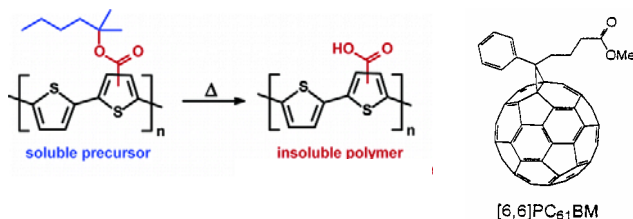
Different approaches (i.e. PhC) are investigated in order to increase light absorption.



PhC in PV CELLS: BULK HETERO JUNCTION



PhC obtained via Pattern Replication In Nonwetting Templates

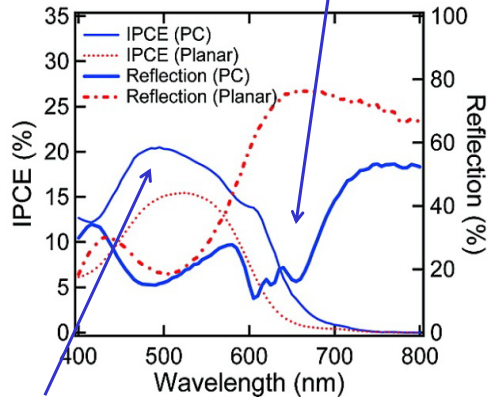




PhC in PV CELLS: BULK HETERO JUNCTION

Nano Lett. 2009, 9, 2742

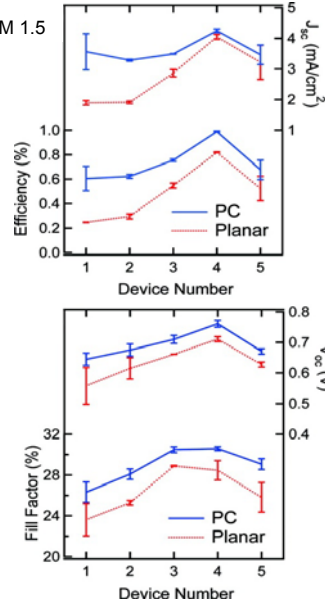
Reduced reflectance → stronger absorption



Increased IPCE (incident photon to current conversion efficiency)

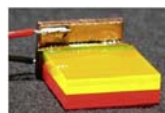
Improved performances are obtained for all relevant cell parameters indicating that both larger absorption and electrical enhancements are achieved

AM 1.5

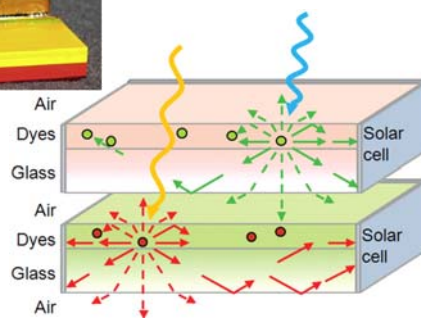


FLUORESCENT CONCENTRATORS

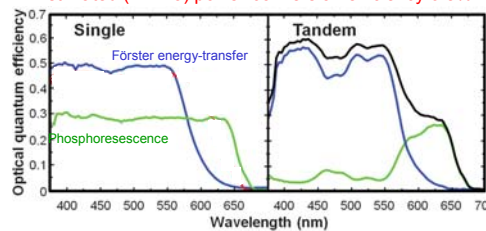
- Fluorescent concentrators (Fluko) are planar waveguides with a thin-organic film coating on the face and inorganic solar cells attached to the edges.
- Light is absorbed by the coating and re-emitted at longer wavelengths into waveguide modes for collection by side solar cells.
- Stacked flukos with spectrally matched solar cells can be obtained.
- Performances of fluko is always limited by self-absorption losses that restrict maximum concentration factors.
- The exploitation of different photophysical processes like Förster energy-transfer, solid-state solvation and phosphorescence enable to overcome self-absorption problem in "conventional flukos".
- In spite of that, 20-30% of emitted radiation is not guided toward solar cells.



Science 321 226 (2008)



Estimated (AM1.5) power-conversion efficiency 6.8%



PhCs ALLOW TO COLLECT NON-GUIDED RADIATION



PhC @ FLUORESCENT CONCENTRATORS

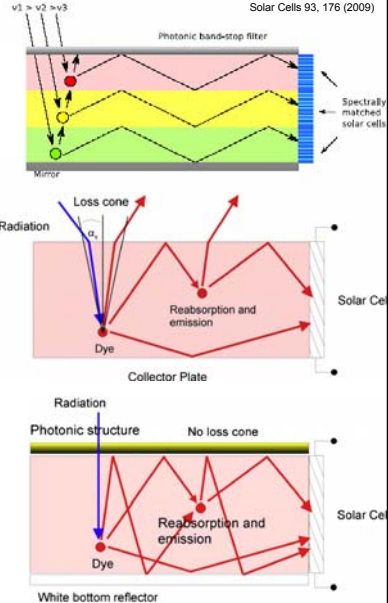
Fluko's key features are a stack of different fluorescent concentrators to use a broad spectral range photonic structures, which increase the fraction of light guided to the edges of the concentrator.

Solar cells are electrically independent each other thus reducing forced series connections.

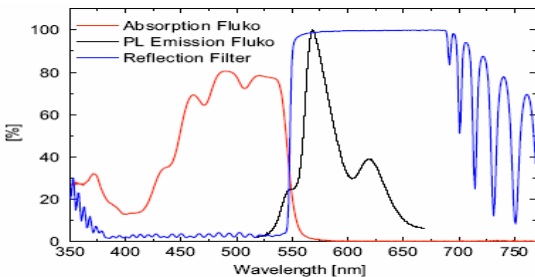
The escape cone of internal total reflection is the major loss mechanism of flukos. Light re-emitted that impinges on the internal surface with an angle greater than the critical one is totally internal reflected

$$\sqrt{1 - \frac{1}{n^2}} \quad \text{For } n=1.6, \text{ 78\% of light is trapped and 22\% get lost}$$

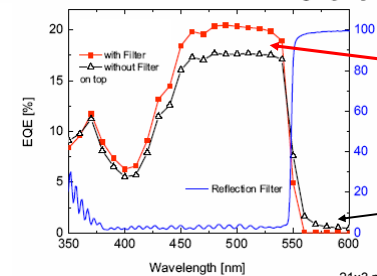
A PhC acting as a stopband reflection filter, which reflects all light in the emission range of the dye, should significantly increase the collection efficiency of the concentrator.



PhC @ FLUORESCENT CONCENTRATORS



$$EQE = \frac{\text{number of harvested electrons}}{\text{number of incident photons}}$$



Strong efficiency increase is achieved in the dye absorption region

Weak efficiency reduction occurs in the high reflectivity spectral region

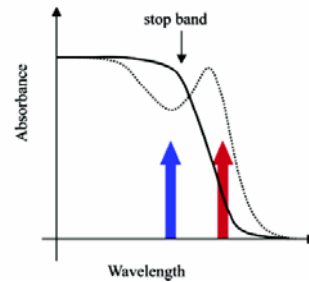
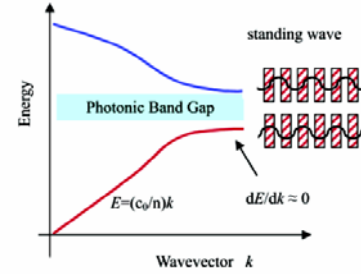
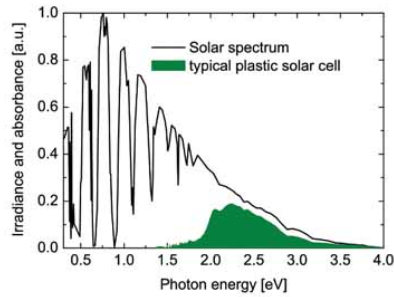
21x3 mm² GaInP solar cell
2x6 cm² fluko
BaSO₄ bottom reflector



INVERSE-OPALS in DSSC

PhC induced properties useful for PV

- Inhibition of spontaneous emission.
- Light localization @ donor/acceptor interface.
- Absorption spectrum extension.
- Improved light harvesting.
- Improved carrier mobility due to ordered percolation path.
- Light insertion into the PV device.



JACS 125, 6306 (03)
J. Phys. Chem. 109, 6334 (05)



INVERSE-OPALS in DSSC

J. AM. CHEM. SOC. 2003, 125, 6306–6310

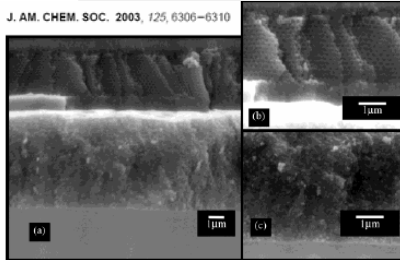
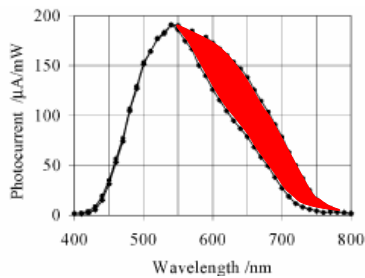
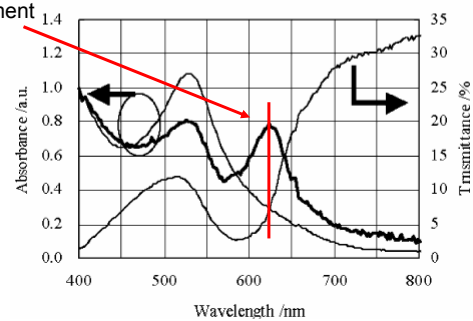
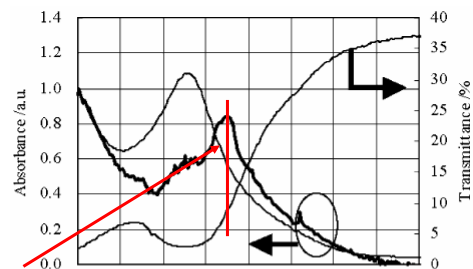


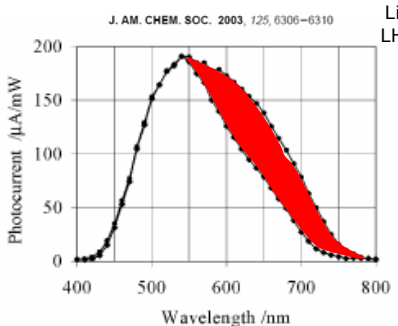
Figure 5. (a) Scanning electron micrograph of a cross section of the bilayer photonic crystal–nano-TiO₂ photoelectrode. The conductive glass is at the top of the image in (a). The photonic crystal layer and the nanocrystalline TiO₂ layer are enlarged in (b) and (c), respectively.



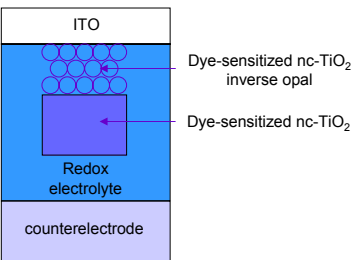
Edge enhancement



INVERSE-OPALS in DSSC



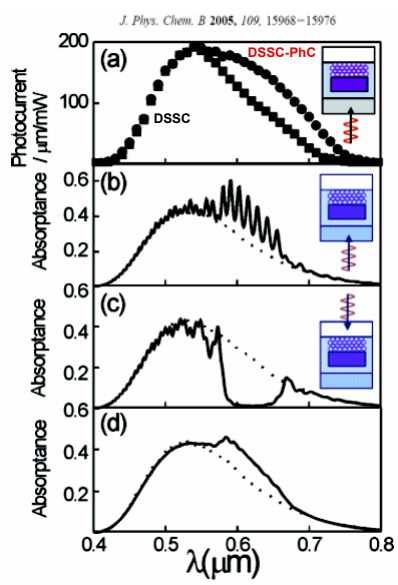
Light harvesting efficiency
 $LHE(\lambda) = \text{absorptance} = I_A/I_0$
 $J_{SC} = \int LHE(\lambda)$



Front illumination:
Light localized by the PhC

Back illumination:
Light reflected by the PhC

Front illumination:
Light localized by the PhC.
Smearing out due to thickness inhomogeneity



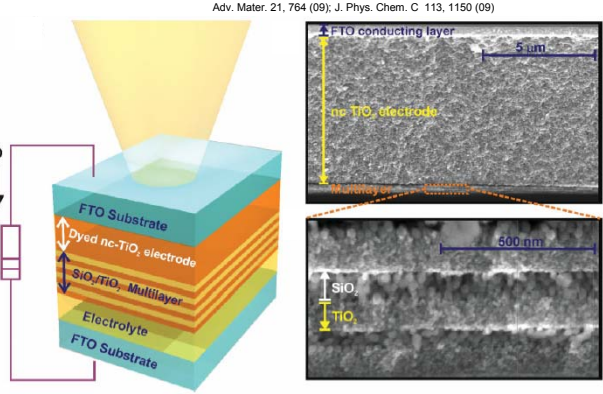
1D-PhC in DSSC

Adv. Mater. 21, 764 (09); J. Phys. Chem. C 113, 1150 (09)

- in order to improve DSSC performances, most efforts are based on using different dyes or ionic conductors. They improve I_{sc} , but also cause a decrease in the V_{oc} and vice versa, due to the sensibility of the charge-transport and recombination dynamics to any alteration of the interfaces present in the cell.
- To enhance the cell efficiency without affecting charge separation and recombination, light-harvesting efficiency have to be improved.
- Reflection of unabsorbed photons back into the film improves the incident-photon-to-current conversion efficiency.
- Unfortunately, some of the most successful approaches developed to improve Si-PV based on the implementation of coherent scattering devices cannot be realized in liquid-semiconductor heterojunction cells.
- The need for an electrical contact between the electrolyte and the sensitized semiconductor slab requires the back reflector to be porous in order to allow a flow of the liquid conductor through it.
- Second, processing of these cells involves deposition of solid layers from colloidal suspensions, which complicates the implementation of quality optical components in the device.
- Inverse opals to dye-sensitized nc-TiO₂ films showed interesting results since IPCE was shown to increase with respect to that of a standard reference cell, at least as a proof of concept even tough no power conversion efficiency improvements have been measured.
- Thick inverse opals (5–10 mm thick) are very likely to have a deleterious effect on charge transport and recombination through the cell, which results in a significant reduction in both the open-circuit photovoltage and the photocurrent in real operation conditions.

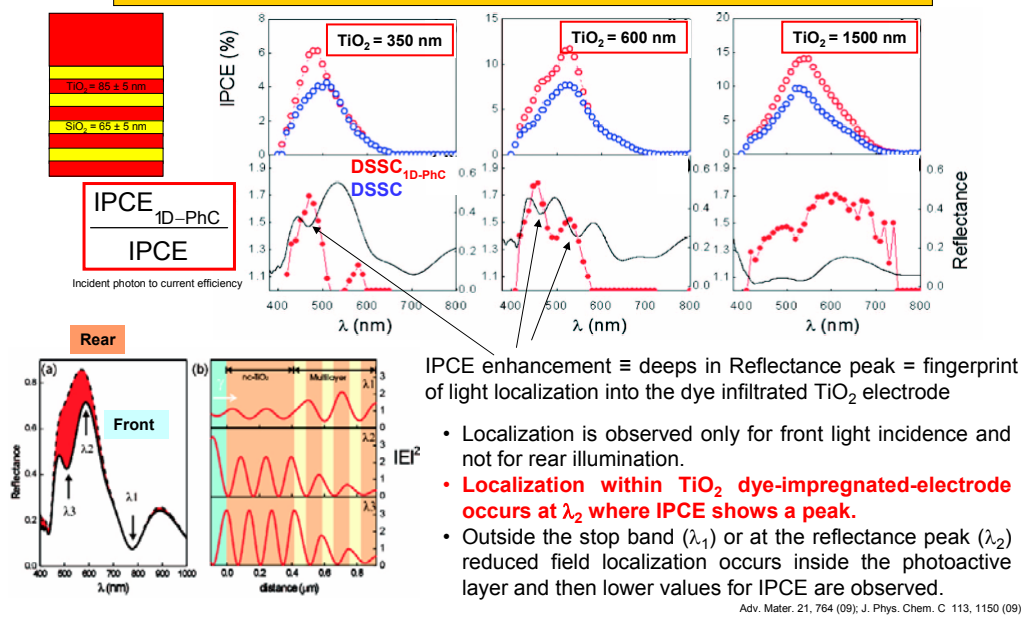
1D-PhC in DSSC

- A novel device structure based on porous 1D-PhC coupled to a dye-sensitized nc-TiO₂ electrode has been proposed.
- This coherent mirror is made by the deposition of alternate layers of SiO₂ and TiO₂ nanoparticles by spin-coating.
- With a thickness of just half a micrometer, the PhC is able to localize incident light within the nc-dyed TiO₂ electrode in a targeted wavelength range.
- Average power conversion efficiencies are improved to between 15 and 30% of the reference value attained for standard electrodes.
- The photogenerated current is greatly improved without altering V_{oc}.
- The transparency of the cell, one of its added values, remains intact, contrary to what happens when scattering layers are employed to improve light harvesting.



Adv. Mater. 21, 764 (09); J. Phys. Chem. C 113, 1150 (09)

1D-PhC in DSSC



Adv. Mater. 21, 764 (09); J. Phys. Chem. C 113, 1150 (09)



CONCLUSIONS

- I hope this lecture might trigger your interest in Photonic Crystals, a new class of materials suitable for controlling light propagation.
- Once again, a multi-cultural approach mixing together fundamental knowledge in chemistry, physics and material science allows to prepare novel materials with unusual properties.